



## GASTRIN RECEPTOR-AVID PEPTIDE CONJUGATES

### CROSS-REFERENCE

This patent application is a continuation-in-part of United States Patent Application Serial No. 09/537,423, filed March 29, 2000, which is a divisional of United States Patent Application Serial No. 09/064,499, filed April 22, 1998 which is a conversion of U.S. Provisional Application Serial No. 60/044,049, filed on April 22, 1997, all of which are incorporated herein by reference.

### GRANT REFERENCE

The research carried out in connection with this invention was supported in part by a grant from the Department of Energy (DOE), grant number DE-FG02-89ER60875, a grant from the U.S. Department of Veterans Affairs Medical Research Division and the Department of Radiology MU-C2-02691. . The Government has certain rights in the invention.

### TECHNICAL FIELD

This invention relates to radionuclide-labeled compounds useful as radiopharmaceuticals. More particularly, the present invention relates to conjugates of bombesin (BBN) analogues and a metal complexing group which, when complexed to a radionuclide, are useful therapeutic and imaging agents for cancer cells that express gastrin releasing peptide (GRP) receptors.

### BACKGROUND OF THE INVENTION

Detection and treatment of cancers using radiopharmaceuticals that selectively target cancers in human patients has been employed for several decades. Unfortunately, only a limited number of site-directed radiopharmaceuticals that exhibit highly specific *in vivo* localization in or near cancer cells are currently in routine use, as being approved by the United States Food and Drug Administration (FDA). There is a great deal of interest in developing new radioactive drugs due to the emergence of more sophisticated biomolecular carriers that have high affinity and high specificity for *in vivo* targeting of tumors. Several types of agents are being developed and have been investigated including monoclonal antibodies (MAbs), antibody fragments ( $F_{AB}$ 's and  $(F_{AB})_2$ 's), receptor-avid peptides [Bushbaum, 1995; Fischman et al., 1993; Schubiger et al. 1996].

The potential utility of using radiolabeled receptor-avid peptides for producing radiopharmaceuticals is best exemplified by  $^{111}\text{In}$ -DTPA-conjugated octreotide (an FDA approved diagnostic imaging agent, Octreoscan®, marketed in the United States. by Mallinckrodt Medical, Inc.) [Lowbertz et al. 1994]. This radiopharmaceutical is an  $^{111}\text{In}$ -DTPA conjugate of Octreotide, a small peptide analogue of the human hormone somatostatin. This drug specifically binds to somatostatin receptors that are over-expressed on neuroendocrine cancers (e.g., carcinoid Ca, neuroblastoma, etc.) as well as others [Krenning et al., 1994]. Since indium-111 ( $^{111}\text{In}$ ) is not the ideal radionuclide for scintigraphic imaging, other somatostatin analogues and other receptor-avid biomolecules that are labeled with  $^{99m}\text{Tc}$  (the optimal radionuclide for diagnostic imaging) are being studied and developed [Eckelman,

1995; Vallabhajosula et al., 1996].

Bombesin (BBN) is a 14 amino acid peptide that is an analogue of human gastrin releasing peptide (GRP) that binds to GRP receptors with high specificity and has an affinity similar to GRP [Davis et al., 1992]. GRP receptors have been shown to be over-expressed or uniquely expressed on several types of cancer cells. Binding of GRP receptor agonists (also autocrine factors) increases the rate of cell division of these cancer cells. For this reason, a great deal of work has been, and is being pursued to develop BBN or GRP analogues that are antagonists [Davis et al., 1992; Hoffken, 1994; Moody et al., 1996; Coy et al., 1988; Cai et al., 1994]. These antagonists are designed to competitively inhibit endogenous GRP binding to GRP receptors and reduce the rate of cancer cell proliferation [Hoffken, 1994]. Treatment of cancers using these antagonists with these non-radioactive peptides requires chronic injection regimens (e.g., daily, using large quantities of the drug).

In designing an effective receptor-avid radiopharmaceutical for use as a diagnostic or therapeutic agent for cancer, it is important that the drug have appropriate *in vivo* targeting and pharmacokinetic properties [Fritzberg et al., 1992; Eckelman et al., 1993]. For example, it is essential that the radiolabeled receptor-avid peptide have high specific uptake by the cancer cells (e.g., via GRP receptors). In addition, it is necessary that once the radionuclide localizes at a tumor site, it must remain there for an extended time to deliver a highly localized radiation dose to the tumor. In order to achieve sufficiently high specific uptake of radiolabeled BBN analogues in tumors, the binding affinity of promising derivatives must be high (i.e.,  $K_d \approx 1-5$  nmolar or less) with prolonged retention of radioactivity [Eckelman et al., 1995; Eckelman, et al., 1993]. Work with  $^{125}\text{I}$ -BBN derivatives has shown, however, that for cancer cells that bind the  $^{125}\text{I}$ -BBN derivatives (whether they be agonists or antagonists), the radioactivity is either washed off or expelled from the cells (*in vitro*) at a rapid rate [Hoffman et al., 1997]. Thus, these types of derivatives have a low probability of remaining "trapped" at the tumor site (*in vivo*) sufficiently long to be effective therapeutic or diagnostic agents.

Developing radiolabeled peptides that are cleared efficiently from normal tissues is also an important and especially critical factor for therapeutic agents. When labeling biomolecules (e.g., MAb,  $F_{AB}$ 's or peptides) with metallic radionuclides (via a chelate conjugation), a large percentage of the metallic radionuclide (in some chemical form) usually becomes "trapped" in either the kidney or liver parenchyma (i.e., is not excreted into the urine or bile) [Duncan et al., 1997; Mattes, 1995]. For the smaller radiolabeled biomolecules (i.e., peptides or  $F_{AB}$ 's), the major route of clearance of activity is through the kidneys which in turn retain high levels of the radioactive metal (i.e., normally  $> 10-15\%$  of the injected dose) [Duncan et al., 1997]. This presents a major problem that must be overcome in the

development of therapeutic agents that incorporate metallic radionuclides, otherwise the radiation dose to the kidneys would be excessive. For example,  $^{111}\text{In}$ -octreotide, the FDA approved diagnostic agent, exhibits high uptake and retention in kidneys of patients [Eckelman et al., 1995]. Even though the radiation dose to the kidneys is higher than desirable, it is tolerable in that it is a diagnostic radiopharmaceutical (it does not emit alpha- or beta-particles), and the renal dose does not produce observable radiation induced damage to the organ.

It has been found that conjugating non-metallated metal chelates to BBN derivatives can form GRP agonists which exhibit binding affinities to GRP receptors that are either similar to or approximately an order of magnitude lower than the parent BBN derivative. [Li et al., 1996a] Our recent results show that it is now possible to add radiometal chelates to BBN analogues, to form conjugates which are agonists, and retain GRP receptor binding affinities that are sufficiently high (i.e., approx. 1-5 nmolar  $K_d$ 's) for further development as potential radiopharmaceuticals. These agonist conjugates are transported intracellularly after binding to cell surface GRP receptors and retained inside of the cells for extended time periods. In addition, *in vivo* studies in normal mice have shown that retention of the radioactive metal in the kidneys was low (i.e., <5%) with the majority of the radioactivity excreted into the urine.

According to one aspect of the present invention, there is provided a BBN conjugate consisting of essentially a radio-metal chelate covalently appended to the receptor binding region of BBN [e.g., BBN(8-14) or BBN(7-14)] to form radiolabeled BBN analogues that have high specific binding affinities with GRP receptors. These analogues are retained for long times inside of GRP expressing cancer cells. Furthermore, their clearance from the bloodstream, into the urine with minimal kidney retention, is efficient. Preferably, the radiometals are selected from  $^{99\text{m}}\text{Tc}$ ,  $^{186/188}\text{Re}$ ,  $^{105}\text{Rh}$ ,  $^{153}\text{Sm}$ ,  $^{166}\text{Ho}$ ,  $^{90}\text{Y}$ ,  $^{199}\text{Au}$ ,  $^{177}\text{Lu}$ ,  $^{149}\text{Pr}$ , or  $^{111}\text{In}$ , all of which hold the potential for diagnostic (i.e.,  $^{99\text{m}}\text{Tc}$  and  $^{111}\text{In}$ ) or therapeutic (i.e.,  $^{186/188}\text{Re}$ ,  $^{105}\text{Rh}$ ,  $^{153}\text{Sm}$ ,  $^{166}\text{Ho}$ ,  $^{90}\text{Y}$ ,  $^{199}\text{Au}$ ,  $^{177}\text{Lu}$ ,  $^{149}\text{Pm}$ ,  $^{166}\text{Dy}$ ,  $^{175}\text{Yb}$ ,  $^{117\text{m}}\text{Sm}$  and  $^{111}\text{In}$ ) utility in cancer patients [Schubiger et al, 1996; Eckelman, 1995; Troutner, 1978].

#### SUMMARY OF THE INVENTION

In accordance with the present invention, there is provided a compound for use as a therapeutic or diagnostic radiopharmaceutical which includes a group which is capable of complexing a metal attached to a moiety capable of binding to a gastrin releasing peptide receptor.

Additionally, in accordance with the present invention, a method for treating a subject having a neoplastic disease which includes the step of administering to the subject an effective amount of a radiopharmaceutical having a metal chelated with a chelating group

attached to a moiety capable of binding to a gastrin releasing peptide receptor on a cancer cell, subsequently intracellularly transported and residualized inside the cell, is disclosed.

Additionally, in accordance with the present invention, a method of forming a therapeutic or diagnostic compound including the step of reacting a metal synthon with a chelating group covalently linked with a moiety capable of binding a gastrin releasing peptide receptor is disclosed.

#### BRIEF DESCRIPTION OF THE DRAWINGS

Other advantages of the present invention will be readily appreciated as the same becomes better understood by reference to the following detailed description when considered in connection with the accompanying drawings wherein:

FIGURE 1 illustrates a radiometal conjugate according to the present invention;

FIGURE 2 is an ORTEP drawing of the  $\{Rh[16]aneS_4-oCl_2\}^+$ , illustrating the crystal structure a Rhodium macrocycle;

FIGURE 3 illustrates a coupling reaction wherein a spacer group is coupled to a bombesin agonist binding moiety;

FIGURE 4 illustrates a coupling reaction for coupling a metal chelate to a peptide;

FIGURE 5 illustrates several iodinated bombesin analogues including their  $IC_{50}$ 's;

FIGURE 6 illustrates several tethered bombesin analogues;

FIGURE 7 illustrates several  $[16]aneS_4$  bombesin analogues;

FIGURE 8 is a graph illustrating  $IC_{50}$  analysis wherein %-I-125-BBN total uptake versus molar concentration of displacing ligand is shown;

FIGURE 9 illustrates several Rhodium- $[16]aneS_4$  bombesin analogues;

FIGURE 10 illustrates an HPLC chromatogram of Rhodium-BBN-37 wherein (A) illustrates  $^{105}RhCl_2$ -BBN-37 and (B) illustrates  $RhCl_2$ -BBN-37;

FIGURE 11 is a graph illustrating  $^{125}I$ -Tyr<sup>4</sup>-bombesin internalization efflux from Swiss 3T3 cells;

FIGURE 12 illustrates I-125 bombesin internalization efflux in I-125 free buffer wherein  $^{125}I$ -Tyr<sup>4</sup>-BBN vs.  $^{125}I$ -Lys<sup>3</sup>-BBN efflux from Swiss 3T3 cells is shown;

FIGURE 13 is a graph illustrating the efflux of  $^{105}Rh$ -BBN-37 from Swiss 3T3 cells;

FIGURE 14 illustrates several  $^{105}Rh$  bombesin analogues including their  $IC_{50}$ 's;

FIGURE 15 is a graph illustrating  $^{105}Rh$ -BBN-61 efflux from Swiss 3T3 cells;

FIGURE 16 is a graph illustrating the efflux of  $^{105}\text{Rh}$ -BBN-22 vs.  $^{105}\text{Rh}$ -BBN-37 from Swiss 3T3 cells;

FIGURE 17 are graphs illustrating Pancreatic CA cell binding wherein (A) illustrates the efflux  $^{125}\text{I}$ -Tyr<sup>4</sup>-BBN from CF PAC1 cells and (B) illustrates the efflux of  $^{105}\text{Rh}$ -BBN-37 from CF PAC1 cells;

FIGURE 18 are graphs illustrating Prostate CA cell binding wherein (A) illustrates the efflux of  $^{125}\text{I}$ -Tyr<sup>4</sup>-BBN from PC-3 cells and (B) illustrates the efflux of  $^{105}\text{Rh}$ -BBN-37 from PC-3 cells;

FIGURE 19 illustrates 5 [16]aneS<sub>4</sub> bombesin analogues which utilize amino acids as Linking Groups;

FIGURE 20 illustrates 4 Rhodium-[16]aneS<sub>4</sub> bombesin analogues and IC<sub>50</sub> values obtained in 3 cell lines;

FIGURE 21 illustrates 3 different N<sub>3</sub>S-BFCA conjugates of BBN(7-14);

FIGURE 22 illustrates on HPLC chromatogram of  $^{99\text{m}}\text{Tc}$ -BBN-122;

FIGURE 23 is a graph illustrating  $^{99\text{m}}\text{Tc}$ -BBN-122 internalization into human prostate cancer cells (PC-3 cells);

FIGURE 24 is a graph illustrating  $^{99\text{m}}\text{Tc}$ -BBN-122 internalization into human pancreatic tumor cells (CFPAC-1 cells);

FIGURE 25 is a graph illustrating  $^{99\text{m}}\text{Tc}$ -RP-414-BBN-42 retention in PC-3 prostate cancer cells;

FIGURE 26 is a graph illustrating  $^{99\text{m}}\text{Tc}$ -42 retention in CFPAC-1 pancreatic cancer cells;

FIGURE 27 illustrates further radiometal conjugates according to the present invention;

FIGURE 28 are HPLC chromatograms of (a) DOTA-BBN[7-14-NH<sub>2</sub>] ( $\lambda = 280$  nm) (b) In-DOTA-BBN[7-14]NH<sub>2</sub> ( $\lambda = 280$  nm) and (c)  $^{111}\text{In}$ -DOTA-BBN[7-14]NH<sub>2</sub> (radiometric);

FIGURE 29 is a graph showing the competitive binding assay of In-DOTA-8-Aoc-BBN[7-14]NH<sub>2</sub> v.  $^{125}\text{I}$ -Tyr<sup>4</sup>-BBN in PC-3 cells;

FIGURE 30 is a graph showing the internalization of  $^{111}\text{In}$ -DOTA-8-Aoc-BBN[7-14]NH<sub>2</sub> in PC-3 cells;

FIGURE 31 is a graph showing the efflux of  $^{111}\text{In}$ -DOTA-8-Aoc-BBN[7-14]NH<sub>2</sub> in PC-3 cells; and

FIGURE 32 is illustrates radiometal conjugate according to the present invention.

## DETAILED DESCRIPTION OF THE INVENTION

According to the present invention, compounds for use as diagnostic and/or therapeutic radiopharmaceuticals include a group capable of complexing a metal attached to a moiety capable of binding to a gastrin releasing peptide (GRP) receptor as shown in Figure

- 5 1. These compounds can be prepared with either a diagnostic radiometal or a therapeutic radiometal thus affording utilities as either a diagnostic agent to identify cancerous tissues within the body using scintigraphic imaging techniques, or a therapeutic agent for the treatment and control of cancerous tissues. The moiety capable of specific binding to the GRP receptor is a GRP agonist. A GRP agonist activates or produces response by the GRP  
10 receptor upon interaction with the GRP receptor and is subsequently internalized inside of the cell by endocytosis. In contrast, a GRP antagonist counteracts the effect of an agonist and is not internalized inside of the cell.

- More specifically, the GRP agonist for the purpose of this invention is a compound such as selected amino acid sequences or peptidomimetics which are internalized  
15 or residualized following binding with high affinity and selectivity to GRP receptors and that can be covalently linked to the metal complexing group. Many examples of specific modifications of the BBN(7-14) or BBN(8-14) that can be made to produce sequences with high antagonistic and agonistic binding affinity for GRP receptors have been reported by numerous investigations [Davis et al., 1992; Hoffken, 1994; Moody et al., 1996; Coy et al.,  
20 1988; Cai et al., 1994; Moody et al., 1995; Leban et al., 1994; Cai et al., 1992].

- In a preferred embodiment of the present invention, the metal complexing group or moiety is a chelating agent or chelator which complexes to metals such as  $^{105}\text{Rh}$ -,  $^{186/188}\text{Re}$ -,  $^{99\text{m}}\text{Tc}$ -,  $^{153}\text{Sm}$ -,  $^{166}\text{Ho}$ -,  $^{90}\text{Y}$ -,  $^{111}\text{In}$ -,  $^{177}\text{Lu}$ -,  $^{149}\text{Pm}$ -,  $^{149}\text{Sm}$  or  $^{199}\text{Au}$ . The chelating agent or chelator is attached or bound to the GRP agonist "binding region" through a spacer to  
25 produce a conjugate that retains its capability for high affinity and specific binding to GRP receptors.

- In a more preferred embodiment of the present invention, the GRP agonist is a bombesin (BBN) analogue and/or a derivative thereof. The BBN derivative or analog thereof preferably contains either the same primary structure of the BBN binding region [i.e.,  
30 BBN(8-14) or BBN(7-14)] or similar primary structures, with specific amino acid substitutions, that will specifically bind to GRP receptors with better or similar binding affinities as BBN alone (i.e.,  $K_d \cong 1\text{-}5\text{ nmolar}$ ). Compounds containing this BBN binding region (or binding moiety), when covalently linked to other groups (e.g., a radiometal chelate), are also referred to as BBN conjugates.

35

In general, the compounds of the present invention have a structure of the general formula:



wherein X is a group capable of complexing a metal, such as a radiometal; Y is a covalent bond on a spacer group; and B is a bombesin agonist binding moiety.

The metal bound to the metal complexing group can be any suitable metal chosen for a specific therapeutic or diagnostic use including transition metals, lanthanides, auger electron emitting isotopes,  $\alpha$ ,  $\beta$  or  $\gamma$  emitting isotopes. Preferably, the metal is a radiometal such as  $^{105}\text{Rh}$ -,  $^{99\text{m}}\text{Tc}$ -,  $^{186/188}\text{Re}$ -,  $^{153}\text{Sm}$ -,  $^{166}\text{Ho}$ -,  $^{111}\text{In}$ -,  $^{90}\text{Y}$ -,  $^{177}\text{Lu}$ -,  $^{149}\text{Pm}$ -,  $^{153}\text{Sm}$ -, and  $^{199}\text{Au}$ - whose chelates can be covalently linked (i.e., conjugated) to the specific BBN binding region via the N-terminal end of the primary binding sequence (e.g., BBN-8 or Trp<sup>8</sup>) as shown in Figure 1.

In a preferred embodiment, the radiometal complexes are positioned by being spaced apart from or remotely from the amino acid Trp<sup>8</sup> by the spacer groups. The spacer groups can include a peptide (i.e.,  $\geq 1$  amino acid in length), a hydrocarbon spacer of  $\text{C}_1\text{-C}_{10}$  or a combination of thereof. Preferably, the hydrocarbon spacer is a  $\text{C}_3\text{-C}_9$  group. The resulting radio-labeled BBN conjugates retain high binding affinity and specificity for GRP receptors and are subsequently internalized inside of the cell.

The BBN conjugates can further incorporate a spacer group or component to couple the binding moiety to the metal chelator (or metal binding backbone) while not adversely affecting either the targeting function of the BBN-binding moiety or the metal complexing function of the metal chelating agent.

The term "spacer group" or "linker" refers to a chemical group that serves to couple the BBN binding moiety to the metal chelator while not adversely affecting either the targeting function of the BBN binding moiety or the metal complexing function of the metal chelator. Suitable spacer groups include peptides (i.e., amino acids linked together) alone, a non-peptide group (e.g., hydrocarbon chain) or a combination of an amino acid sequence and a non-peptide spacer. The type of spacer group used in most of the experimental studies described below in the Examples section were composed of a combination of L-glutamine and hydrocarbon spacers. A pure peptide spacer could consist of a series of amino acids (e.g., diglycine, triglycine, gly-gly-glu, gly-ser-gly, etc.), in which the total number of atoms between the N-terminal residue of the BBN binding moiety and the metal chelator in the polymeric chain is  $\leq 12$  atoms.

The spacer can also include a hydrocarbon chain [i.e.,  $\text{R}_1\text{-(CH}_2\text{)}_n\text{-R}_2$ ] wherein  $n$  is 0-10, preferably  $n = 3$  to 9,  $\text{R}_1$  is a group (e.g.,  $\text{H}_2\text{N-}$ ,  $\text{HS-}$ ,  $\text{-COOH}$ ) that can be used as a site for covalently linking the ligand backbone or the preformed metal chelator or metal

complexing backbone; and R<sub>2</sub> is a group that is used for covalent coupling to the N-terminal NH<sub>2</sub>-group of the BBN binding moiety (e.g., R<sub>2</sub> is an activated COOH group). Several chemical methods for conjugating ligands (i.e., chelators) or preferred metal chelates to biomolecules have been well described in the literature [Wilbur, 1992; Parker, 1990; Hermanson, 1996; Frizberg et al., 1995]. One or more of these methods could be used to link either the uncomplexed ligand (chelator) or the radiometal chelate to the spacer group or to link the spacer group to the BBN(8-14) derivatives. These methods include the formation of acid anhydrides, aldehydes, arylisothiocyanates, activated esters, or N-hydroxysuccinimides [Wilbur, 1992; Parker, 1990; Hermanson, 1996; Frizberg et al., 1995].

The term "metal complexing chelator" refers to a molecule that forms a complex with a metal atom that is stable under physiological conditions. That is, the metal will remain complexed to the chelator backbone *in vivo*. More particularly, a metal complexing chelator is a molecule that complexes to a radionuclide metal to form a metal complex that is stable under physiological conditions and which also has at least one reactive functional group for conjugation with the BBN agonist binding moiety. Metal complexing chelators can include monodentate and polydentate chelators [Parker, 1990; Frizberg et al., 1995; Lister-James et al., 1997; Li et al., 1996b; Albert et al., 1991; Pollak et al., 1996; de Jong et al., 1997; Smith et al., 1997] and include the DOTA chelators discussed in more detail below. Metal complexing chelators include tetradentate metal chelators which can be macrocyclic and have a combination of four nitrogen and/or sulfur metal-coordinating atoms [Parker et al., 1990; Li et al., 1996b] and are designated as N<sub>4</sub>, S<sub>4</sub>, N<sub>3</sub>S, N<sub>2</sub>S<sub>2</sub>, NS<sub>3</sub>, etc. as shown in Figure 2. A number of suitable multidentate chelators that have been used to conjugate proteins and receptor-avid molecules have been reported [Frizberg et al., 1995; Lister-James et al., 1997; Li et al., 1996b; Albert et al., 1991; Pollak et al., 1996; de Jong et al., 1997] and include the DOTA chelators discussed in more detail below. These multidentate chelators can also incorporate other metal-coordinating atoms such as oxygen and phosphorous in various combinations. The metal binding complexing moiety can also include "3+1" chelators [Seifert et al., 1998].

For diagnostic purposes, metal complexing chelators preferably include chelator backbones for complexing the radionuclide metals <sup>99m</sup>Tc and <sup>111</sup>In. For therapeutic purposes, metal complexing chelators preferably include chelator backbones that complex the beta particle emitting radionuclide metals including <sup>105</sup>Rh, <sup>186/188</sup>Re, <sup>153</sup>Sm, <sup>90</sup>Y, <sup>166</sup>Ho, <sup>199</sup>Au, <sup>177</sup>Lu, <sup>111</sup>In, <sup>166</sup>Dy, <sup>175</sup>Yb and <sup>149</sup>Pm [Schubiger et al., 1996; Hoffken, 1994].

As was briefly described above, the term "bombesin agonist" or "BBN agonist" refers to compounds that bind with high specificity and affinity to GRP receptors, and upon binding to the GRP receptor, are intracellularly internalized. Suitable compounds



include peptides, peptidomimetics and analogues and derivatives thereof. In particular, previous work has demonstrated that the region on the BBN peptide structure required for binding to GRP receptors spans from residue 8 through 14 [Davis et al., 1992; Hoffken, 1994; Moody et al., 1996; Coy, 1988; Cai et al., 1994]. The presence of methionine (Met) at position BBN-14 will generally confer agonistic properties while the absence of this residue at BBN-14 generally confers antagonistic properties [Hoffken, 1994].

It is well documented in the art that there are a few and selective number of specific amino acid substitutions in the BBN (8-14) binding region (e.g., D-Ala<sup>11</sup> for L-Gly<sup>11</sup> or D-Trp<sup>8</sup> for L-Trp<sup>8</sup>), which can be made without decreasing binding affinity [Leban et al., 1994; Qin et al., 1994; Jensen et al., 1993]. In addition, attachment of some amino acid chains or other groups to the N-terminal amine group at position BBN-8 (i.e., the Trp<sup>8</sup> residue) can dramatically decrease the binding affinity of BBN analogues to GRP receptors [Davis et al., 1992; Hoffken, 1994; Moody et al., 1996; Coy, et al., 1988; Cai et al., 1994]. In a few cases, it is possible to append additional amino acids or chemical moieties without decreasing binding affinity. The effects of conjugating various side chains to BBN-8 on binding affinity, therefore, is not predicable.

The BBN conjugates of the present invention can be prepared by various methods depending upon the selected chelator. The peptide portion of the conjugate can be most conveniently prepared by techniques generally established and known in the art of peptide synthesis, such as the solid-phase peptide synthesis (SPPS) approach. Solid-phase peptide synthesis (SPPS) involves the stepwise addition of amino acid residues to a growing peptide chain that is linked to an insoluble support or matrix, such as polystyrene. The C-terminal residue of the peptide is first anchored to a commercially available support with its amino group protected with an N-protecting agent such as a t-butyloxycarbonyl group (tBoc) or a fluorenylmethoxycarbonyl (Fmoc) group. The amino protecting group is removed with suitable deprotecting agents such as TFA in the case of tBOC or piperidine for Fmoc and the next amino acid residue (in N-protected form) is added with a coupling agent such as dicyclocarbodiimide (DCC). Upon formation of a peptide bond, the reagents are washed from the support. After addition of the final residue, the peptide is cleaved from the support with a suitable reagent such as trifluoroacetic acid (TFA) or hydrogen fluoride (HF).

The spacer groups and chelator components are then coupled to form a conjugate by reacting the free amino group of the Trp<sup>8</sup> residue of the BBN binding moiety with an appropriate functional group of the chelator, metal chelator or spacer group, such as a carboxyl group or activated ester.

The BBN conjugate can also incorporate a metal complexing chelator backbone that is peptidic and compatible with solid-phase peptide synthesis. In this case, the

chelator backbone can be added to the BBN binding moiety in the same manner as described above or, more conveniently, the metal complexing chelator backbone coupled to the BBN binding moiety can be synthesized *in toto* starting from the C-terminal residue of the peptide and ending with the N-terminal residue of the metal complexing chelator structure.

The chelator backbones used in accordance with the present invention are commercially available or they could be made by methods similar to those outlined in the literature [Frizberg et al., 1995; Lister-James et al., 1997; Li et al., 1996b; Albert et al., 1991; Pollak et al., 1996; de Jong et al., 1997; Smith et al., 1997; Seifert et al., 1998]. Attachment of the spacer groups to functionalizable atoms appended to the ligand backbone can be performed by standard methods known to those skilled in the art. For example, the HOBt/HBTU activated -COOH group on 5-aminovaleric acid (5-AVA) was reacted with the N-terminal amine on Gln<sup>7</sup> to produce an amide linkage as shown in Figure 3. Similarly, the -COOH group attached to the characterized [16]aneS<sub>4</sub> ligand was conjugated to the amine group on the hydrocarbon spacer (shown below) by reaction of the HOBt/HBTU activated carboxyl group appended to the [16]aneS<sub>4</sub> macrocycle with the terminal amine group on 5-AVA to form BBN-37 as shown in Figure 4. Other standard conjugation reactors that produce covalent linkages with amine groups can also be used [Wilbur, 1992; Parker, 1990].

The chelating framework, conjugated via Trp<sup>8</sup>, that complexes the radiometals should form a 1:1 chelator to metal ratio. Since <sup>99m</sup>Tc has a short half-life (6 hour) and is a diagnostic radionuclide, the method of forming the <sup>99m</sup>Tc-BBN analogues should permit complexation (either directly or by transmetallation) of <sup>99m</sup>Tc to the conjugated chelating framework in a one-step, high yield reaction (exemplified below in the Experimental Section).

In contrast, the longer half lives of the therapeutic radionuclides (e.g., <sup>105</sup>Rh, <sup>186/188</sup>Re, <sup>153</sup>Sm, <sup>166</sup>Ho, <sup>90</sup>Y, <sup>177</sup>Lu, <sup>149</sup>Pm, <sup>199</sup>Au, <sup>111</sup>In, <sup>177</sup>Lu) permit formation of the corresponding radiolabeled BBN analogues by either a one step high yield complexation step or by performing a <sup>105</sup>Rh-, <sup>186/188</sup>Re-, <sup>153</sup>Sm, <sup>166</sup>Ho, <sup>90</sup>Y, <sup>177</sup>Lu, <sup>111</sup>In or <sup>149</sup>Au chelate synthon followed by conjugation of the preformed complex to the N-terminal end of the BBN binding moiety. In all cases, the resulting specific activity of the final radiolabeled BBN derivative must be high (i.e., > 1Ci/ $\mu$ mole).

#### Re- and Tc-conjugates

Re and Tc are both in row VIIB of the Periodic Table and they are chemical congeners. Thus, for the most part, the complexation chemistry of these two metals with ligand frameworks that exhibit high *in vitro* and *in vivo* stabilities are the same [Eckelman, 1995]. Many <sup>99m</sup>Tc or <sup>186/188</sup>Re complexes, which are employed to form stable radiometal complexes with peptides and proteins, chelate these metals in their +5 oxidation state [Lister-

James et al., 1997]. This oxidation state makes it possible to selectively place  $^{99m}\text{Tc}$ - or  $^{186/188}\text{Re}$  into ligand frameworks already conjugated to the biomolecule, constructed from a variety of  $^{99m}\text{Tc(V)}$  and/or  $^{186/188}\text{Re(V)}$  weak chelates (e.g.,  $^{99m}\text{Tc}$ - glucoheptonate, citrate, gluconate, etc.) [Eckelman, 1995; Lister-James et al., 1997; Pollak et al., 1996]. Tetradentate ligand frameworks have been shown to form well-defined, single chemical species in high specific activities when at least one thiol group or at least one hydroxymethylene phosphine group is present on the ligand backbone [Smith et al., 1997].

Ligands which form stable  $\text{Tc(V)}$  or  $\text{Re(V)}$  tetradentate complexes containing, but not limited to, amino N-atoms, amido-N-atoms, carboxy-O-atoms and thioether-S-atoms, are donor atoms that can also be present [Eckelman, 1995; Fritzberg et al., 1992; Parker, 1990; Frizberg et al., 1995; Pollak et al., 1996; Seifert et al., 1998]. Depending upon the mix of donor atoms (groups), the overall complex charge normally ranges from -1 to +1.

Incorporation of the metal within the conjugate can be achieved by various methods commonly known in the art of coordination chemistry. When the metal is technetium-99m, the following general procedure can be used to form a technetium complex. A peptide-chelator conjugate solution is formed by initially dissolving the conjugate in water or in an aqueous alcohol such as ethanol. The solution is then degassed to remove oxygen. When an -SH group is present in the peptide, the thiol protecting group(s) are removed with a suitable reagent, for example with sodium hydroxide, and are then neutralized with an organic acid such as acetic acid (pH 6.0-6.5). In the labeling step, sodium pertechnetate obtained from a molybdenum generator is added to a solution of the conjugate with a sufficient amount of a reducing agent, such as stannous chloride, to reduce technetium and is either allowed to stand at room temperature or is heated. The labeled conjugate can be separated from the contaminants  $^{99m}\text{TcO}_4^-$  and colloidal  $^{99m}\text{TcO}_2$  chromatographically, for example with a C-18 Sep Pak cartridge [Millipore Corporation, Waters Chromatography Division, 34 Maple Street, Milford, Massachusetts 01757].

In an alternative method, the labeling can be accomplished by a transchelation reaction. The technetium source is a solution of technetium complexed with labile ligands facilitating ligand exchange with the selected chelator. Examples of suitable ligands for transchelation includes tartrate, citrate, gluconate, and heptagluconate. It will be appreciated that the conjugate can be labeled using the techniques described above, or alternatively, the chelator itself may be labeled and subsequently coupled to the peptide to form the conjugate; a process referred to as the "prelabeled chelate" method.

When labeled with diagnostically and/or therapeutically useful metals, peptide-chelator conjugates or pharmaceutically acceptable salts, esters, amides, and prodrugs of the present invention can be used to treat and/or detect cancers, including



5 The therapeutic application of these compounds can be defined either as an agent that will be used as a first line therapy in the treatment of cancer, as combination therapy where these radiolabeled agents could be utilized in conjunction with adjuvant chemotherapy, and as the matched pair therapeutic agent. The matched pair concept refers to one compound which can serve as both a diagnostic and a therapeutic agent depending on the radiometal with the appropriate chelate selected and can be understood in connection with the data set forth below.

10 Radioisotope therapy involves the administration of a radiolabeled compound in sufficient quantity to damage or destroy the targeted tissue. After administration of the compound (by e.g. intravenous or intraperitoneal injection), the radiolabeled pharmaceutical localizes preferentially at the disease site (in this instance, tumor tissue that expresses the GRP-receptor). Once localized, the radiolabeled compound then damages or destroys the diseased tissue with the energy that is released during the radioactive decay of the isotope that is administered.

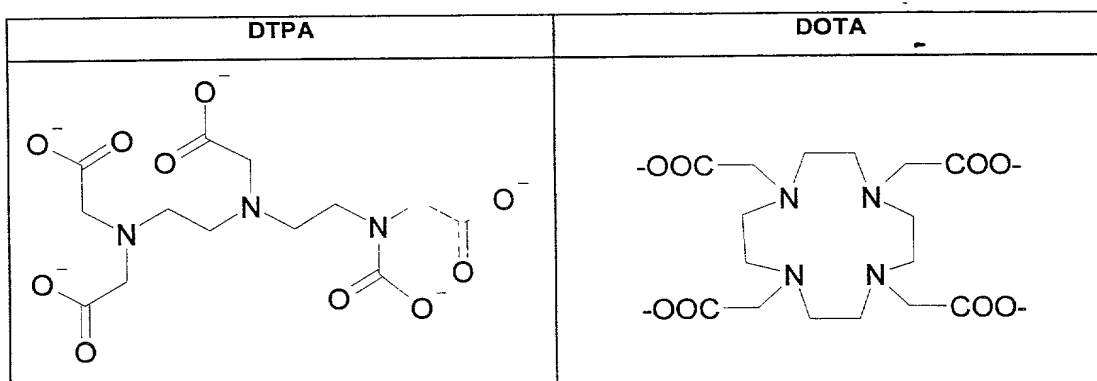
15 The design of a successful radiotherapeutic involves several critical factors:

1. selection of an appropriate targeting group to deliver the radioactivity to the disease site;
2. selection of an appropriate radionuclide that releases sufficient energy to damage that disease site, without substantially damaging adjacent normal tissues; and
- 20 3. selection of an appropriate combination of the targeting group and the radionuclide without adversely affecting the ability of this conjugate to localize at the disease site. For radiometals, this often involves a chelating group that coordinates tightly to the radionuclide, combined with a linker that couples said chelate to the targeting group, and that affects the overall biodistribution of the compound to maximize uptake in target tissues and minimizes uptake in normal, non-target organs.

25 The present invention provides radiotherapeutic agents that satisfy all three of the above criteria, through proper selection of targeting group, radionuclide, metal chelate and linker.

30 Radiotherapeutic agents may contain a chelated 3+ metal ion from the class of elements known as the lanthanides (elements of atomic number 57-71) and their analogs (i.e.  $M^{3+}$  metals such as yttrium and indium). Typical radioactive metals in this class include the isotopes 90-Yttrium, 111-Indium, 149-Promethium, 153-Samarium, 166-Dysprosium, 166-Holmium, 175-Ytterbium, and 177-Lutetium. All of these metals (and others in the lanthanide series) have very similar chemistries, in that they remain in the +3 oxidation state, and prefer

to chelate to ligands that bear hard (oxygen/nitrogen) donor atoms, as typified by derivatives of the well known chelate DTPA (Diethylenetriaminepentaacetic acid) and polyaza-polycarboxylate macrocycles such as DOTA (1,4,7,10-tetrazacyclododecane-N, N',N'',N'''-tetraacetic acid and its close analogs. The structures of these chelating ligands, in their fully deprotonated form are shown below.



These chelating ligands encapsulate the radiometal by binding to it *via* multiple nitrogen and oxygen atoms, thus preventing the release of free (unbound) radiometal into the body. This is important, as *in vivo* dissociation of +3 radiometals from their chelate can result in uptake of the radiometal in the liver, bone and spleen [Brechtel MW, Gansow OA, "Backbone-substituted DTPA ligands for <sup>90</sup>Y radioimmunotherapy", Bioconj. Chem. 1991; 2: 187-194; Li, WP, Ma DS, Higginbotham C, Hoffman T, Ketrang AR, Cutler CS, Jurisson, SS, "Development of an in vitro model for assessing the in vivo stability of lanthanide chelates." Nucl. Med. Biol. 2001; 28(2): 145-154; Kasokat T, Urich K. *Arzneim.-Forsch.* "Quantification of dechelation of gadopentetate dimeglumine in rats". 1992; 42(6): 869-76]. Unless one is specifically targeting these organs, such non-specific uptake is highly undesirable, as it leads to non-specific irradiation of non-target tissues, which can lead to such problems as hematopoietic suppression due to irradiation of bone marrow.

For radiotherapy applications, forms of the DOTA chelate [Tweedle MF, Gaughan GT, Hagan JT, "1-Substituted-1,4,7-triscarboxymethyl-1,4,7,10-tetraazacyclododecane and analogs." US Patent 4,885,363, Dec. 5, 1989] are particularly preferred, as the DOTA chelate is expected to de-chelate less in the body than DTPA or other linear chelates.

General methods for coupling DOTA-type macrocycles to targeting groups through a linker (e.g. by activation of one of the carboxylates of the DOTA to form an active ester, which is then reacted with an amino group on the linker to form a stable amide bond),

are known to those skilled in the art. (See e.g. Tweedle et al. US Patent 4,885,363). Coupling can also be performed on DOTA-type macrocycles that are modified on the backbone of the polyaza ring.

The selection of a proper nuclide for use in a particular radiotherapeutic application depends on many factors, including:

a. **Physical half-life** - This should be long enough to allow synthesis and purification of the radiotherapeutic construct from radiometal and conjugate, and delivery of said construct to the site of injection, without significant radioactive decay prior to injection. Preferably, the radionuclide should have a physical half-life between about 0.5 and 8 days.

b. **Energy of the emission(s) from the radionuclide** - Radionuclides that are particle emitters (such as alpha emitters, beta emitters and Auger electron emitters) are particularly useful, as they emit highly energetic particles that deposit their energy over short distances, thereby producing highly localized damage. Beta emitting radionuclides are particularly preferred, as the energy from beta particle emissions from these isotopes is deposited within 5 to about 150 cell diameters. Radiotherapeutic agents prepared from these nuclides are capable of killing diseased cells that are relatively close to their site of localization, but cannot travel long distances to damage adjacent normal tissue such as bone marrow.

c. **Specific activity (i.e. radioactivity per mass of the radionuclide)** - Radionuclides that have high specific activity (e.g. generator produced 90-Y, 111-In, 177-Lu) are particular preferred. The specific activity of a radionuclide is determined by its method of production, the particular target that is used to produce it, and the properties of the isotope in question.

Many of the lanthanides and lanthanoids include radioisotopes that have nuclear properties that make them suitable for use as radiotherapeutic agents, as they emit beta particles. Some of these are listed in the table below.

Isotope	Half -Life (days)	Max $\beta$ - energy (MeV)	Gamma energy (keV)	Approximate range of $\beta$ - particle (cell diameters)
149-Pm	2.21	1.1	286	60
153-Sm	1.93	0.69	103	30
166-Dy	3.40	0.40	82.5	15
166-Ho	1.12	1.8	80.6	117
175-Yb	4.19	0.47	396	

177-Lu	6.71	0.50	208	20
90-Y	2.67	2.28	-	150
111-In	2.810	Auger electron emitter	173, 247	< 5 $\mu$ m

Pm:promethium, Sm:samarium, Dy:dysprosium, Ho:holmium, Yb:ytterbium, Lu:lutetium, Y:yttrium, In:Indium

Methods for the preparation of radiometals such as beta-emitting lanthanide radioisotopes are known to those skilled in the art, and have been described elsewhere [e.g. Cutler C S, Smith CJ, Ehrhardt GJ.; Tyler TT, Jurisson SS, Deutsch E. "Current and potential therapeutic uses of lanthanide radioisotopes." Cancer Biother. Radiopharm. 2000; 15(6): 531-545]. Many of these isotopes can be produced in high yield for relatively low cost, and many (e.g. 90-Y, 149-Pm, 177-Lu) can be produced at close to carrier-free specific activities (i.e. the vast majority of atoms are radioactive). Since non-radioactive atoms can compete with their radioactive analogs for binding to receptors on the target tissue, the use of high specific activity radioisotope is important, to allow delivery of as high a dose of radioactivity to the target tissue as possible.

Radiotherapeutic derivatives of the invention containing beta-emitting isotopes of rhenium (186-Re and 188-Re) are also particularly preferred. Proper dose schedules for the radiotherapeutic compounds of the present invention are known to those skilled in the art. The compounds can be administered using many methods which include, but are not limited to, a single or multiple IV or IP injections, using a quantity of radioactivity that is sufficient to cause damage or ablation of the targeted GRP-R bearing tissue, but not so much that substantive damage is caused to non-target (normal tissue). The quantity and dose required is different for different constructs, depending on the energy and half-life of the isotope used, the degree of uptake and clearance of the agent from the body and the mass of the tumor. In general, doses can range from a single dose of about 30-50 mCi to a cumulative dose of up to about 3 Curies.

The radiotherapeutic compositions of the invention can include physiologically acceptable buffers, and can require radiation stabilizers to prevent radiolytic damage to the compound prior to injection. Radiation stabilizers are known to those skilled in the art, and may include, for example, para-aminobenzoic acid, ascorbic acid, gentistic acid and the like.

The following examples are presented to illustrate specific embodiments and demonstrate the utility of the present invention.



## Experimental Section

EXAMPLE 1: Synthesis and in vitro binding assessment of synthetic BBN analogues employing hydrocarbon chain spacers

### 5                   A. Synthesis:

Many BBN analogues were synthesized by Solid Phase Peptide Synthesis (SPPS). Each peptide was prepared by SPPS using an Applied Biosystems Model 432A peptide synthesizer. After cleavage of each BBN analogue from the resin using Trifluoroacetic acid (TFA), the peptides were purified by C18 reversed-phase HPLC using a Vydac HS54  
10       column and CH<sub>3</sub>CN/H<sub>2</sub>O containing 0.1% TFA as the mobile phase. After collection of the fraction containing the desired BBN peptide (approx. 80-90% yield in most cases), the solvent was evaporated. The identity of each BBN peptide was confirmed by FAB-mass spectrometry, Department of Chemistry - Washington University, St. Louis, MO.

Various amino acid sequences (in some cases including different chemical  
15       moieties) were conjugated to the N-terminal end of the BBN binding region (i.e., to BBN-8 or Trp8). BBN analogue numbers 9,15,15i, 16, 16i and 18 were synthesized as examples of N-terminal modified peptides as shown in Figure 5.

Various tethered N-terminal (via Trp8) BBN analogues were also synthesized by SPPS as exemplified by BBN-40, BBN-41, BBN-42, BBN-43, BBN-44, BBN-45, and BBN-  
20       49 as shown in Figure 6. In these particular tethered peptides, a Glu residue was attached to Trp8 followed by attachment of fmoc protected terminal amine groups separated from a -COOH group by 3-, 4-, 5-, 6-, 8- and 11-carbon chain (CH) spacers (Figure 6). These fmoc protected acids were added as the terminal step during the SPPS cycle. As described previously, each of the BBN analogues was purified by reversed-phase HPLC and  
25       characterized by high resolution Mass Spectroscopy. Peptide 49 employed only glutamine as the spacer group.

The [16]aneS4 macrocyclic ligand was conjugated to selected tethered BBN analogues shown in Figure 6. The -OCH<sub>2</sub>COOH group on the [16]aneS4 macrocycle derivative was activated via HOBt/HBTU so that it efficiently formed an amide bond with the  
30       terminal NH<sub>2</sub> group on the spacer side arm (following deprotection). The corresponding [16]aneS<sub>4</sub> tethered BBN derivatives were produced and examples of 4 of these derivatives (i.e., BBN-22, -37, -46 and -47) are shown in Figure 7. As previously described, each [16]aneS<sub>4</sub> BBN derivative was purified by reversed phase HPLC and characterized by FAB Mass Spectroscopy.

### 35                   B. In Vitro Binding Affinities

The binding affinities of the synthetic BBN derivatives were assessed for GRP receptors on Swiss 3T3 cells and, in some cases, on a variety of human cancer cell

lines, that express GRP receptors. The IC<sub>50</sub> value of each derivative was determined relative to (i.e., in competition with) <sup>125</sup>I-Tyr<sub>4</sub>-BBN (the K<sub>d</sub> for <sup>125</sup>I-Tyr<sub>4</sub>-BBN for GRP receptors in Swiss 3T3 cells is reported to be 1.6±0.4 nM) [Zuehl et al., 1991]. The cell binding assay methods used to measure the IC<sub>50</sub>'s is standard and used techniques previously reported [Jensen et al., 1993; Cai et al., 1994; Cai et al., 1992]. The methods used for determining IC<sub>50</sub>'s for all GRP receptor binding compounds on all cell lines was similar. The specific method used to measure IC<sub>50</sub>'s on Swiss 3T3 cells is briefly described as follows:

Swiss 3T3 mouse fibroblasts are grown to confluence in 48 well microtiter plates. An incubation media was prepared consisting of HEPES (11.916g/l), NaCl (7.598 g/l), KCl (0.574 g/l), MgCl<sub>2</sub> (1.106 g/l), EGTA (0.380 g/l), BSA (5.0 g/l), chymostatin (0.002 g/l), soybean trypsin inhibitor (0.200 g/l), and bacitracin (0.050 g/l). The growth media was removed, the cells were washed twice with incubation media, and incubation media was returned to the cells. <sup>125</sup>I-Tyr<sub>4</sub>-BBN (0.01 uCi) was added to each well in the presence of increasing concentrations of the appropriate competitive peptide. Typical concentrations of displacing peptide ranged from 10<sup>-12</sup> to 10<sup>-5</sup> moles of displacing ligand per well. The cells were incubated at 37°C for forty minutes in a 95%O<sub>2</sub>/5%CO<sub>2</sub> humidified environment. At forty minutes post initiation of the incubation, the medium was discarded, and the cells were washed twice with cold incubation media. The cells were harvested from the wells following incubation in a trypsin/EDTA solution for five minutes at 37°C. Subsequently, the radioactivity, per well, was determined and the maximum % total uptake of the radiolabeled peptide was determined and normalized to 100%.

#### C. Results of Binding Affinity Measurements:

The IC<sub>50</sub> values measured for the BBN derivatives synthesized in accordance with this invention showed that appending a peptide side chain and other moieties via the N-terminal BBN-8 residue (i.e., Trp<sup>8</sup>) produced widely varying IC<sub>50</sub> values. For example, see IC<sub>50</sub> values shown for BBN 11, 15i, 16i, and 18 in Figures 5 and 8. The observations are consistent with previous reports showing highly variable IC<sub>50</sub> values when derivatizing BBN(8-13) or BBN(8-14) with a predominantly short chain of amino acid residues [Hoffken, 1994]. In contrast, when a hydrocarbon spacer of 3- to 11-carbons was appended between BBN(7-14) and the [16]aneS<sub>4</sub> macrocycle, the IC<sub>50</sub>'s were found to be surprisingly relatively constant and in the 1-5 nM range. The following IC<sub>50</sub> values were obtained from the unmetallated compounds BBN-22, -37, -46, and -47 (structures shown in Figure 7).

<u>COMPOUND</u>	<u>IC<sub>50</sub> (nM)</u>
BBN-22	3.01 ± 0.21
BBN-37	1.79 ± 0.09

BBN-46	2.34 ± 0.53
BBN-47	4.19 ± 0.91

These data suggest that using relatively simple spacer groups to extend ligands some distance from the BBN binding region [e.g., BBN(8-14)] can produce derivatives that maintain binding affinities in the 1-5 nmolar range.

#### D. Cell Binding Studies With Metal Complexes:

5           The following IC<sub>50</sub> values were obtained for the metallated Rhodium complexes shown on Figure 9.

<u>COMPOUND</u>	<u>IC<sub>50</sub> (nM)</u>
RhCl <sub>2</sub> BBN-22	37.5 ± 10.5
RhCl <sub>2</sub> BBN -37	4.76 ± 0.79
RhCl <sub>2</sub> BBN -46	3.38 ± 0.69

10       The results illustrated in Figure 9 show that when the RhCl<sub>2</sub>-[16]aneS<sub>4</sub> complexes separated from Trp<sup>8</sup> by only a glutamine (Glu<sup>7</sup>), the IC<sub>50</sub> of this conjugate (i.e., Rh-BBN-22) was 37.5 nM. However, when a five (5) carbon spacer or an eight (8) carbon spacer was present (i.e., Rh-BBN-37 and Rh-BBN-47), the IC<sub>50</sub>'s remained below 5 nM. These data demonstrate that a straight chain spacer (along with glu<sup>7</sup>) to move the +1 charged Rh-S<sub>4</sub>-chelate away from the BBN binding region will result in a metallated BBN analogue with sufficiently high binding affinities to GRP receptors for *in vivo* tumor targeting applications.

#### E. <sup>105</sup>Radiolabeled BBN Analogues:

15       The <sup>105</sup>Rh conjugates of BBN-22, BBN-37, BBN-46 and BBN-47 were synthesized using a <sup>105</sup>Rh-chloride reagent from the Missouri University Research Reactor (MURR). This reagent was obtained as <sup>105</sup>Rh-chloride, a no-carrier-added (NCA) product, in 0.1-1M HCl. The pH of this reagent was adjusted to 4-5 using 0.1-1.0 M NaOH dropwise and it was added to approximately 0.1 mg of the [16]aneS<sub>4</sub>-conjugated BBN derivatives in 20   0.9% aqueous NaCl and 10% ethanol. After the sample was heated at 80°C for one hour, the <sup>105</sup>Rh-BBN analogues were purified using HPLC. In each case, a NCA or high specific activity product was obtained since the non-metallated S<sub>4</sub>-BBN conjugates eluted at a retention time well after the <sup>105</sup>Rh-BBN conjugates eluted. For example, the retention time of <sup>105</sup>Rh-BBN-37 was 7.1 minutes while BBN-37 eluted at 10.5 minutes from a C-18-reversed 25   phase column eluted with CH<sub>3</sub>CN/H<sub>2</sub>O containing 0.1% TFA as shown in Figure 10A-B.

#### EXAMPLE 2: Retention of <sup>105</sup>Rh-BBN Analogues in Cancer Cells

Once the radiometal has been specifically "delivered" to cancer cells (e.g., employing the BBN binding moiety that specifically targets GRP receptors on the cell surface), it is necessary that a large percentage of the "delivered" radioactive atoms remain

associated with the cells for a period time of hours or longer to make an effective radiopharmaceutical for effectively treating cancer. One way to achieve this association is to internalize the radiolabeled BBN conjugates within the cancer cell after binding to cell surface GRP receptors.

In the past, all of the work with synthetic-BBN analogues for treatment of cancers focused on synthesizing and evaluating antagonists [Davis et al., 1992; Hoffken, 1994; Moody et al., 1996; Coy et al., 1988; Cai et al., 1994; Moody et al., 1995; Leban et al., 1994; Cai et al., 1992]. After evaluating synthetic BBN analogues that would be predicted to be either agonists or antagonists, applicants found that derivatives of BBN(8-14) (i.e., those with the methionine or amidated methionine at BBN-14) are rapidly internalized (i.e., in less than two minutes) after binding to the cell surface GRP receptors. Several radiolabeled BBN(8-14) analogues that were studied to determine their internalization and intracellular trapping efficiencies were radioiodinated (i.e.,  $^{125}\text{I}$ ) derivatives. The results of these studies demonstrated that despite rapid internalization after  $^{125}\text{I}$ -labeled BBN analogue binding to GRP receptors in Swiss 3T3 cells, the  $^{125}\text{I}$  was rapidly expelled from the cells [Hoffman et al., 1997] as shown in Figure 11. Thus, these  $^{125}\text{I}$ -BBN derivatives were not suitable for further development.

In contrast, the  $^{105}\text{Rh}$ -BBN(8-14) derivatives that bind to GRP receptors are not only rapidly internalized, but there is a large percentage of the  $^{105}\text{Rh}$  activity that remains trapped within the cells for hours (and in some cell lines > twenty four hours). This observation indicates that these radiometallated BBN derivatives have real utility as radiopharmaceuticals for *in vivo* targeting of neoplasms expressing GRP receptors.

Experiments designed to determine the fraction of a radiotracer internalized within cells were performed by adding excess  $^{125}\text{I}$ - or  $^{105}\text{Rh}$ -BBN derivatives to the cell incubation medium. After establishment of equilibrium after a forty minute incubation, the media surrounding the cells was removed and the cells were washed with fresh media containing no radioactivity. After washing, the quantity of radioactivity associated with the cells was determined (i.e., total counts per minute (TCPM) of  $^{125}\text{I}$  or  $^{105}\text{Rh}$  associated with the cells). The cells were then incubated in a 0.2M acetic acid solution (pH 2.5) which caused the surface proteins (incl., GRP receptors) to denature and release all surface bound radioactive materials. After removing this buffer and washing, the cells were counted again. The counts per minute (c.p.m.) associated with the cells at that point were only related to the  $^{125}\text{I}$  or  $^{105}\text{Rh}$  that remained trapped inside of the cells.

To determine intracellular retention, a similar method was employed. However, after washing the cells with fresh (non-radioactive) incubation media, the cells were incubated in the fresh media at different time periods after washing away all extracellular  $^{125}\text{I}$ -

or  $^{105}\text{Rh}$ -BBN analogues. After each time period, the methods used to determine TOTAL c.p.m. and intracellular c.p.m. after washing with a 0.2M acetic acid solution at pH 2.5 were the same as described above and the percent  $^{125}\text{I}$  or  $^{105}\text{Rh}$  remaining trapped inside of the cells was calculated. Figure 12 is a graph of results of efflux experiments using Swiss 3T3 cells with  $^{125}\text{I}$ -Lys<sup>3</sup>-BBN. The results show that there is rapid efflux of the  $^{125}\text{I}$  from inside of these cells with less than 50% retained at fifteen minutes and by sixty minutes, less than 20% remained as shown in Figure 12.

In contrast, studies with all of the  $^{105}\text{Rh}$ -[16]aneS<sub>4</sub>-BBN agonist derivatives that are internalized inside of the cells showed substantial intracellular retention of  $^{105}\text{Rh}$  by the GRP receptor expressing cells. For example, results of studies using  $^{105}\text{Rh}$ -BBN-37 (see Figure 9) in conjunction with Swiss 3T3 cells showed that approximately 50% of the  $^{105}\text{Rh}$  activity remains associated with the cells at sixty minutes post-washing and approximately 30% of  $^{105}\text{Rh}$  remained inside of the cells after four hours as shown in Figure 13. Note that at least 5% of the  $^{105}\text{Rh}$  is surface bound at  $\geq$  sixty minutes.

The  $^{105}\text{Rh}$ -BBN derivatives shown in Figure 9 all have an amidated methionine at position BBN-14 and are expected to be agonists [Jensen et al., 1993]. Therefore, they would be predicted to rapidly internalize after binding to GRP receptors on the cell surface [Reile et al., 1994; Bjisterbosch et al., 1995; Smythe et al., 1991], which was confirmed by applicants' data. Referring to Figure 14,  $^{105}\text{Rh}$ -BBN-61, a BBN analogue with no amino acid at position BBN-14 (i.e., a  $^{105}\text{Rh}$ -BBN(8-13) derivative), was synthesized and studied. This BBN analogue has a high bonding affinity (i.e.,  $\text{IC}_{50} = 4.1 \text{ nM}$ ). This type of derivative is expected to be an antagonist and as such will not internalize [Jensen et al., 1993; Smythe et al., 1991]. Results of efflux studies with  $^{105}\text{Rh}$ -BBN-61 using Swiss 3T3 cells showed that immediately following washing with fresh incubation buffer (i.e.,  $t=0$ ), essentially all of the  $^{105}\text{Rh}$  associated with these cells is on the cell surface, as expected. Furthermore, after only one hour of incubation, less than 10% remained associated with these cells in any fashion (comparing the results with the antagonist (see Figure 15) to those of the agonist (see Figure 16)). These data indicate that  $^{105}\text{Rh}$ -antagonists with structures similar to the  $^{105}\text{Rh}$ -BBN agonists (i.e., those shown in Figure 9) are not good candidates for development of radiopharmaceuticals since they are neither trapped in nor on the GRP receptor expressing cells to nearly the same extent as the radiometallated BBN agonists.

#### EXAMPLE 3: Human Cancer Cell Line Studies

*In vitro* cell binding studies of  $^{105}\text{Rh}$ -BBN-37 with two different human cancer cell lines that express GRP receptors (i.e., CF-PAC1 and PC-3 cell lines), which are tumor cells derived from patients with prostate CA and pancreatic CA, as shown in Figures 17A-B and 18A-B, respectively ) were performed. Results of these studies demonstrated

consistency with  $^{105}\text{Rh}$ -BBN-37 binding and retention studies using Swiss 3T3 cells.

Specifically, the binding affinity of Rh-BBN-37 was high (i.e.,  $\text{IC}_{50} \cong 7 \text{ nM}$ ) with both human cancer cell lines as shown in Table 1. In addition, in all cells, the majority of the  $^{105}\text{Rh}$ -BBN-37 was internalized and perhaps a major unexpected result was that the retention of the  $^{105}\text{Rh}$ -tracer inside of the cells was significantly better than retention in Swiss 3T3 cells as shown in Figures 17 and 18. For example, it is particularly remarkable that the percentage of  $^{105}\text{Rh}$ -BBN-37 that remained associated with both the CFPAC-1 and PC-3 cell line was  $>80\%$  at two hours after removing the extracellular activity by washing with fresh incubation buffer (see Figures 17 and 18).

#### 10 EXAMPLE 4: *IN VIVO* STUDIES

Biodistribution studies were performed by intravenous (I.V.) injection of either  $^{105}\text{Rh}$ -BBN-22 or  $^{105}\text{Rh}$ -BBN-37 into normal mice. In these studies, unanesthetized CF-1 mice (15-22g, body wt.) were injected I.V. via the tail vein with between one (1) to five (5)  $\mu\text{Ci}$  (37-185 KBq) of the  $^{105}\text{Rh}$ -labeled agent. Organs, body fluids and tissues were excised from animals sacrificed at 30, 60 and 120 minutes post-injection (PI). The tissues were weighed, washed in saline (when appropriate) and counted in a NaI well counter. These data were then used to determine the percent injected dose (% ID) in an organ or fluid and the %ID per gram. The whole blood volume of each animal was estimated to be 6.5 percent of the body weight. Results of these studies are summarized in Tables 2 and 3.

Results from these studies showed that both the  $^{105}\text{Rh}$ -BBN-22 and  $^{105}\text{Rh}$ -BBN-37 were cleared from the blood stream, predominantly via the kidney into the urine. Specifically,  $68.4 \pm 6.6\%$  and  $62.3 \pm 5.8\%$  of the ID was found in urine at two hours PI of  $^{105}\text{Rh}$ -BBN-22 and  $^{105}\text{Rh}$ -BBN-37, respectively (see Tables 2 and 3). An unexpected finding was that the % ID of  $^{105}\text{Rh}$  that remained deposited in the kidneys of these animals was only  $2.4 \pm 0.6\%$  ID and  $4.6 \pm 1.3\%$  ID at two hours PI of  $^{105}\text{Rh}$ -BBN-22 and  $^{105}\text{Rh}$ -BBN-37 (see Tables 2 and 3). This is much less than would be expected from previously reported data where radiometallated peptides and small proteins have exhibited renal retention of the radiometal that is  $> 10\%$  ID and usually much  $> 10\%$  [Duncan et al., 1997]. The reason for reduced renal retention of  $^{105}\text{Rh}$ -BBN analogues is not known, however, this result demonstrates a substantial improvement over existing radiometallated peptides.

Biodistribution studies also demonstrated another important *in vivo* property of these radiometallated BBN analogues. Both  $^{105}\text{Rh}$ -BBN-22 and  $^{105}\text{Rh}$ -BBN-37 are efficiently cleared from organs and tissues that do not express GRP receptors (or those that do not have their GRP-receptors accessible to circulating blood). The biodistribution studies in mice demonstrated specific uptake of  $^{105}\text{Rh}$ -BBN-22 and  $^{105}\text{Rh}$ -BBN-37 in the pancreas while other non-excretory organs or tissues (i.e., heart, brain, lung, muscle, spleen) exhibited

little or no uptake or retention (Tables 2 and 3). Both  $^{105}\text{Rh}$ -BBN-22 and  $^{105}\text{Rh}$ -BBN-37 were removed from the blood stream by both the liver and kidneys with a large fraction of the  $^{105}\text{Rh}$  removed by these routes being excreted into the intestines and the bladder, respectively. It is important to note that the % ID/gm in the pancreas of  $^{105}\text{Rh}$ -BBN-22 and  $^{105}\text{Rh}$ -BBN-37 was  $3.9 \pm 1.3$  % and  $9.9 \pm 5.4$  %, respectively at 2 hour, PI. Thus, the ratios of % ID/gm of  $^{105}\text{Rh}$ -BBN-22 in the pancreas relative to muscle and blood were 16.2 and 7.6, respectively. The ratios of % ID/gm of  $^{105}\text{Rh}$ -BBN-37 in the pancreas relative to muscle and blood were 25.4 and 29.1, respectively. These data demonstrated selective *in vivo* targeting of these radiometallated BBN analogues to cells expressing GRP receptors [Zhu et al., 1991; Qin et al., 1994] and efficient clearance from non-target tissues. If cancer cells that express GRP receptors are present in the body, these results indicate radiometallated BBN analogues will be able to target them with a selectivity similar to the pancreatic cells.

A comparison of the pancreatic uptake and retention of  $^{105}\text{Rh}$ -BBN-22 with  $^{105}\text{Rh}$ -BBN-37 demonstrated that  $^{105}\text{Rh}$ -BBN-37 deposits in the pancreas with a 2-fold better efficiency than  $^{105}\text{Rh}$ -BBN-22 (i.e.,  $3.6 \pm 1.2$  % ID and  $2.3 \pm 1.0$  % ID) for  $^{105}\text{Rh}$ -BBN-37 at one and two hours PI, respectively, vs.  $1.2 \pm 0.5$  % ID and  $1.0 \pm 0.1$  % ID for  $^{105}\text{Rh}$ -BBN-22 at one and two hours PI). This data is consistent with the >2-fold higher uptake and retention of  $^{105}\text{Rh}$ -BBN-37 found in the *in vitro* studies shown in Figure 16.

Example 5: Synthesis and *in vitro* binding measurement of synthetic BBN conjugate analogues employing amino acid chain spacers

#### A. Synthesis

Five BBN analogues were synthesized by SPPS in which between 2 to 6 amino acid spacer groups were inserted to separate a  $\text{S}_4$ -macrocyclic chelator from the N-terminal  $\text{trp}^8$  on BBN(8-14) (Figure 19). Each peptide was prepared by SPPS using an Applied Biosystems Model 432A peptide synthesizer. After cleavage of each BBN analogue from the resin using Trifluoroacetic acid (TFA), the peptides were purified by  $\text{C}_{18}$  reversed-phase HPLC using a Vydac HS54 column and  $\text{CH}_3\text{CN}/\text{H}_2\text{O}$  containing 0.1% TFA as the mobile phase. After collection of the fraction containing the desired BBN peptide, the solvent was evaporated. The identity of each BBN peptide was confirmed by FAB-mass spectrometry (Department of Chemistry - Washington University, St. Louis, MO).

Various amino acid sequences (in some cases containing different R group moieties) were conjugated to the N-terminal end of the BBN binding region (i.e., to BBN-8 or  $\text{Trp}^8$ ). BBN analogue numbers 96, 97, 98, 99 and 101 were synthesized as examples of N-terminal modified peptides in which the [16]ane $\text{S}_4$  macrocycle BFCA was separated from  $\text{trp}^8$  on BBN(8-14) by various amino acid sequences as shown in Figure 19.

The [16]aneS<sub>4</sub> macrocyclic ligand was conjugated to selected tethered BBN analogues. The -OCH<sub>2</sub>COOH group on the [16]aneS<sub>4</sub> macrocycle derivative was activated via HOBt/HBTU so that it efficiently formed an amide bond with the terminal NH<sub>2</sub> group on the spacer side arm (following deprotection). The corresponding [16]aneS<sub>4</sub> tethered BBN derivatives were produced and examples of 5 of these derivatives (i.e., BBN-96, 97, 98, 99 and 101) are shown in Figure 19. As previously described, each [16]aneS<sub>4</sub> BBN derivative was purified by reversed phase HPLC and characterized by FAB Mass Spectroscopy.

#### B. *In Vitro* Binding Affinities

The binding affinities of the synthetic BBN derivatives were assessed for GRP receptors on Swiss 3T3 cells, PC-3 cells and CF PAC-1 cells. The IC<sub>50</sub>'s of each of derivative were determined relative to (i.e., in competition with) <sup>125</sup>I-Tyr<sup>4</sup>-BBN. The cell binding assay methods used to measure the IC<sub>50</sub>'s is standard and was used by techniques previously reported [Jensen et al., 1993; Cai et al., 1992; Cai et al., 1994]. The methods used for determining IC<sub>50</sub>'s with all BBN analogue binding to GRP receptors present on all three cell lines were similar. The specific method used to measure IC<sub>50</sub>'s on Swiss 3T3 cells is briefly described as follows:

Swiss 3T3 mouse fibroblasts are grown to confluence in 48 well microliter plates. An incubation media was prepared consisting of HEPES (11.916g/l), NaCl (7.598 g/l), KCl (0.574 g/l), MgCl<sub>2</sub> (1.106 g/l), EGTA (0.380 g/l), BSA (5.0 g/l), chymostatin (0.002 g/l), soybean trypsin inhibitor (0.200 g/l), and bacitracin (0.050 g/l). The growth media was removed, the cells were washed twice with incubation media, and incubation media was returned to the cells. <sup>125</sup>I-Tyr<sup>4</sup>-BBN (0.01 μCi) was added to each well in the presence of increasing concentrations of the appropriate competitive peptide. Typical concentrations of displacing peptide ranged from 10<sup>-12</sup> to 10<sup>-5</sup> moles of displacing ligand per well. The cells were incubated at 37°C for forty minutes in a 95% O<sub>2</sub>/5% CO<sub>2</sub> humidified environment. At forty minutes post initiation of the incubation, the medium was discarded, and the cells were washed twice with cold incubation media. The cells were harvested from the wells following incubation in a trypsin/EDTA solution for five minutes at 37°C. Subsequently, the radioactivity, per well, was determined and the maximum % total uptake of the radiolabeled peptide was determined and normalized to 100%. A similar procedure was used in performing cell binding assays with both the PC-3 and CF<sub>a</sub>-PAC-1 human cancer cell lines.

#### C. Results of Binding Affinity Measurements

The IC<sub>50</sub> values measured for the BBN derivatives synthesized in accordance with this invention showed that appending a chelator via amino acid chain spacer groups via the N-terminal BBN-8 residue (i.e., Trp<sup>8</sup>) produced a variation of IC<sub>50</sub> values. For example, see IC<sub>50</sub> values shown for BBN 96, 97, 98 and 101 in Figure 19. The observations are



consistent with previous reports showing variable  $IC_{50}$  values when derivatizing BBN(8-13) with a predominantly short chain of amino acid residues [Hoffken, 1994]. When the amino acid spacer groups used in BBN-98, 99 and 101 were appended between BBN(7-14) and the [16]aneS<sub>4</sub> macrocycle, the  $IC_{50}$ 's were found to be surprisingly constant and in the 1-6 nM range for all three cell lines (i.e., see  $IC_{50}$  values shown in Figure 19). These data suggest that using relatively simple spacer groups composed entirely of selected amino acid sequences to extend ligands some distance from the BBN region [e.g., BBN(8-14)] can produce derivatives that maintain binding affinities in the 1-6 nmolar range.

#### D. Cell Binding Studies with Rh-BBN-Conjugates

Results illustrated in Figure 20 show that when the corresponding RhCl<sub>2</sub> [16]aneS<sub>4</sub> complex was separated from Trp<sup>8</sup> on BBN(8-14) by the four different amino acid spacer groups (see Figure 20), the  $IC_{50}$ 's of all four analogues (i.e., BBN-97, -98, -99, -101) were between 0.73 and 5.29 nmolar with GRP receptors on the PC-3 and CF PAC-1 cell lines. The  $IC_{50}$ 's for these same Rh-BBN conjugates were somewhat higher with the Swiss 3T3 cell line (Figure 20). These data demonstrate that amino acid chain with spacer groups used to move the +1 charged Rh-S<sub>4</sub>-chelate away from the BBN binding region will result in a metallated BBN analogue with sufficiently high binding affinities to GRP receptors for *in vivo* tumor targeting applications.

EXAMPLE 6: Synthesis and *in vitro* binding assessment of a <sup>99m</sup>Tc-labeled synthetic BBN analogue

#### A. Synthesis

Several tetradentate chelating frameworks have been used to form stable <sup>99m</sup>Tc or <sup>188</sup>Re labeled peptide and protein conjugates [Eckelman, 1995; Li et al., 1996b; Parker, 1990; Lister-James et al., 1997]. Many of these ligand systems contain at least one thiol (-SH) donor group to maximize rates of formation and stability (both *in vitro* and *in vivo*) of the resultant Tc(V) or Re(V) complexes [Parker, 1990; Eckelman, 1995]. Results from a recent report indicates that the bifunctional chelating agent (BFCA) (dimethylglycyl-L-seryl-L-cysteinyglycinamide (N3S-BFCA) is capable of forming a well-defined complex with ReO<sup>3+</sup> and TcO<sup>3+</sup> [Wong et al., 1997]. Since this ligand framework can be synthesized by SPPS techniques, this N3S-BFCA was selected for use in forming of Tc-<sup>99m</sup>-BBN-analogue conjugates. Three different N3S-BFCA conjugates of BBN(7-14) were synthesized (BBN-120, -121 and -122) as shown in Figure 21 by SPPS. BBN-120, BBN-121 and BBN-122 represent a series of analogues where the N3S-BFCA is separated from the BBN(7-14) sequence by a 3, 5 and 8 carbon spacer groups (Figure 21). Each peptide was synthesized and purified using the SPPS and chromatographic procedures outlined in Example 1. The

thiol group on cysteine was protected using the ACM group, which is not cleaved during cleavage of these BBN-conjugates from the resin using TFA. The identity of BBN-120, -121 and -122 was confirmed by FAB mass spectrometry. Synthesis and purification of the N3S-BFCA could also be readily accomplished using SPPS methods, followed by HPLC purification (see Example 1). The ACM group was used to protect the thiol group on cysteine during synthesis and cleavage from the resin.

#### B. In Vitro Binding Affinities

Synthesis of  $^{99m}\text{Tc}$ -BBN-122 (Figure 22) was prepared by two methods [i.e., (1) by transchelation of  $^{99m}\text{TcO}_3$  from  $^{99m}\text{Tc}$ -gluconate or (2) by formation of the "preformed"  $^{99m}\text{Tc}$ -BFCA complex followed by  $-\text{COOH}$  activation with tetrafluorophenyl and subsequent reaction with the C5-carbon spacer group appended to BBN(7-14)]. In both cases, the  $^{99m}\text{Tc}$ -labeled peptide formed is shown in Figure 22. The structure of this  $\text{Tc}$ -BBN-122 conjugate was determined by using non-radioactive  $\text{Re}$  (the chemical congener of  $\text{Tc}$ ). In these studies, the "preformed"  $\text{ReO}_3$  complex with the N3S-BFCA was prepared by reduction of  $\text{ReO}_4^-$  with  $\text{SnCl}_2$  in the presence of excess N3S-BFCA dissolved in sodium phosphate buffered water at pH 6-6.5 by a method previously published [Wong et al., 1997]. After purification of the  $\text{ReO}$ -N3S-BFCA complex, the structure of this chelate was shown (by Mass-Spect) to be identical to that previously reported [Wong et al., 1997].

The  $\text{ReO}$ -N3S-BFCA complex was converted to the activated trifluorophenyl (TFP) ester by adding 10 mg of the complex to 6 mg (dry) EDC and the 50  $\mu\text{l}$  of TFP. After the solution was vortexed for one minute,  $\text{CH}_3\text{CN}$  was added until disappearance of cloudiness. The solution was incubated for one hour at RT and purified by reversed-phase HPLC. To prepare the  $\text{ReO}$ -N3S-BFCA complex BBN-122 conjugate (Figure 22), one  $\mu\text{l}$  of the HPLC fraction containing the  $\text{ReO}$ -N3S-BFCA complex was added to a solution containing 1 mg of the C8-tethered BBN(7-14) peptide in 0.2 N  $\text{NaHCO}_3$  at pH 9.0. After incubation of this solution for one hour at RT, the sample was analyzed and purified by reversed-phase HPLC. The yield of  $\text{Re}$ -BBN-122 was approximately 30-35%.

The method for preparation of the corresponding  $^{99m}\text{Tc}$ -BBN-122 conjugate, using the "preformed"  $^{99m}\text{TcO}$ -N3S-BFCA complex, was the same as described above with the "preformed"  $\text{ReO}$ -N3S-BFCA complex. In this case,  $^{99m}\text{TcO}_4^-$ , from a  $^{99}\text{Mo}/^{99m}\text{Tc}$  generator, was reduced with an aqueous saturated stannous tartrate solution in the presence of excess N3S-BFCA. The yields of the  $^{99m}\text{Tc}$ -BBN-122 product using this "preformed" method were approximately 30-40%. Reversed phase HPLC analysis of the  $^{99m}\text{Tc}$ -BBN-

122, using the same gradient elution program<sup>1</sup> as used for analysis of the Re-BBN-122 conjugate, showed that both the 99mTc-BBN-122 and 188Re-BBN-122 had the same retention time (i.e., 14.2-14.4 min) (See Figure 22). This provides strong evidence that the structure of both the 99mTc-BBN-122 and Re-BBN-122 are identical.

The binding affinities of BBN-122 and Re-BBN-122 were assessed for GRP receptors on Swiss 3T3 cells, PC-3 cells and CFPAC-1 cells that express GRP receptors. The IC<sub>50</sub>'s of each derivative were determined relative to (i.e., in competition with) 125I-Tyr4-BBN (the K<sub>d</sub> for 125I-Tyr4-BBN for GRP receptors in Swiss 3T3 cells is reported to be 1.6±0.4nM) [Zhu et al., 1991]. The cell binding assay methods used to measure the IC<sub>50</sub>'s is standard and was used by techniques previously reported [Leban et al., 1994; Cai et al., 1994; Cai et al., 1992]. The methods used for determining IC<sub>50</sub>'s with all GRP receptor binding of GRP receptors on all cell lines was similar and has been described previously for the other BBN-analogues and Rh-BBN analogues described in this document.

#### C. Results of Binding Affinity Measurements

The IC<sub>50</sub> values measured for BBN-122 and Re-BBN-122 synthesized in accordance with this invention showed that appending an 8-carbon hydrocarbon chain spacer linked to the N3S1-BFCA and the corresponding Re complex (i.e., Trp8) produced BBN conjugates with IC<sub>50</sub> values in a 1-5 nmolar range (See Table A). When 99mTc-BBN-122 was incubated with these same cells, it was shown that ≥ nmolar concentrations of BBN displaced this 99mTc conjugate by > 90%. This result demonstrates that 99mTc-BBN-122 has high and specific binding affinity for GRP receptors. These data suggest that using relatively simple spacer groups to extend the N3S ligand framework and the corresponding Tc-or Re-N3S1, complexes some distance from the BBN binding region can produce derivatives that maintain binding affinities in the 1-5 nmolar range.

TABLE A.

Summary of IC<sub>50</sub> values for GRP receptor binding for the non-metallated BBN-122 conjugate or the Re-BBN-122 conjugate in two cell lines (PC-3 and CF-PAC-1 cell lines that express GRP receptors). The IC<sub>50</sub> values were measured using cell binding assays relative to 125I-Tyr4-BBN.

<sup>1</sup> Gradient elution program used in these studies was as follows.

Flow 1.5 ml/minute

Solvent A = HO with 0.1% TFA

Solvent B = CHCN with 0.1% TFA

Time (minutes)	%A/%B
0	95/5
25	30/70
35	95/5

Conjugate	IC50 (nmolar)	
	PC-3	CF-PAC1
BBN-122	$3.59 \pm 0.75$ (n=6)	$5.58 \pm 1.92$ (n=14)
Re-BBN-122	$1.23 \pm 0.56$ (n=12)	$1.47 \pm 0.11$ (n=6)

EXAMPLE 7: Retention of  $^{99m}\text{Tc}$ -BBN-122 in Human Cancer Cells PC-3 and CF-PAC-1 cells)

5                   Once the radiometal has been specifically "delivered" to cancer cells (e.g., employing the BBN binding moiety that specifically targets GRP receptors on the cell surface), it is necessary that a large percentage of the "delivered" radioactive atoms remain associated with the cells for a period time of hours or longer to make an effective radiopharmaceutical for effectively treating cancer. One way to achieve this association is to  
10                   internalize the radiolabeled BBN conjugates within the cancer cell after binding to cell surface GRP receptors.

                  Experiments designed to determine the fraction  $^{99m}\text{Tc}$ -BBN-122 internalized within cells were performed by the same method previously described for  $^{105}\text{Rh}$ -BBN-37. Briefly, excess  $^{99m}\text{Tc}$ -BBN-122 was added to PC-3 or CFPAC-1 cell incubation media and  
15                   allowed to establish equilibrium after a forty minute incubation. The media surrounding the cells was removed and the cells were washed with fresh media containing no radioactivity. After washing, the quantity of radioactivity associated with the cells was determined (i.e., total counts per minute  $^{99m}\text{Tc}$  associated with cells). The PC-3 and CFPAC-1 cells were then  
20                   incubated in a 0.2M acetic acid solution (pH2.5) which caused the surface proteins (including GRP receptors) to denature and release all surface bound radioactive materials. After removing this buffer and washing, the cells were counted again. The counts per minute (c.p.m.) associated with the cells at that point were only related to the  $^{99m}\text{Tc}$  that remained trapped inside of the PC-3 or CFPAC-1 cells.

                  To determine intracellular retention of  $^{99m}\text{Tc}$  activity, a similar method was  
25                   employed. However, after washing the cells with fresh (non-radioactive) incubation media, the cells were incubated in the fresh media at different time period after washing away all extracellular  $^{99m}\text{Tc}$ -BBN-122. After each time interval, the methods used to determine total c.p.m. and intracellular c.p.m. by washing with a 0.2M acetic acid solution at pH 2.5.

Studies with the 99mTc-BBN-122 agonist show that it is internalized inside of the PC-3 and CFPAC-1 cells (Figures 23-26) and that substantial intracellular retention of 99mTc by the GRP receptor expressing cells occurs. For example, results of studies using 99mTc-BBN-122 in conjunction with PC-3 cells showed a high rate of internalization (Figure 23) and that approximately 75% of the 99mTc activity remains associated with the cells at ninety minutes post-washing (Figure 25). Almost all of this 99mTc cell-associated activity is inside of the PC-3 cells. Similar results were also found with the CFPAC 1 cells where there is also a high rate of 99mTc-BBN-122 internalization (Figure 24) and relatively slow efflux of 99mTc from the cells (i.e., 50-60% retention at 120 minutes post-washing (Figure 26).

The 99mTc-BBN-122 peptide conjugate shown in Figure 22 has an amidated methionine at position BBN-14 and is expected to be an agonist [Jensen et al., 1993]. Therefore, it would be predicted to rapidly internalize after binding to GRP receptors on the cell surface [Bjisterbosch et al., 1995; Smythe et al., 1991], which is confirmed by applicants' data in Figure 23-26.

#### EXAMPLE 8: In Vivo Studies

Biodistribution studies were performed by intravenous (I.V.) injection of 99mTc-BBN-122 into normal mice. In these studies, unanesthetized CF-1 mice (15-22g, body wt.) were injected I.V. via the tail vein with between one (1) to five (5)  $\mu$ Ci (37-185 KBq) of 99mTc-BBN-122. Organs, body fluids and tissues were excised from animals sacrificed at 0.5, 1, 4 and 24 hours post-injection (PI). The tissues were weighed, washed in saline (when appropriate) and counted in a NaI well counter. These data were then used to determine the percent injected dose (% ID) in an organ or fluid and the % ID per gram. The whole blood volume of each animal was estimated to be 6.5 percent of the body weight. Results of these studies are summarized in Tables B and C.

Results from these studies showed that 99mTc-BBN-122 is cleared from the blood stream predominantly via the hepatobiliary pathway showing about 35% of the 99mTc-activity cleared via the kidney into the urine. Specifically,  $33.79 \pm 1.76\%$  of the ID was found in urine at one hour PI (Table B). The retention of 99mTc activity in the kidneys and liver is very low (Table B). This is much less than would be expected from previously reported data where radiometallated peptides and small proteins have exhibited renal retention of the radiometal that is  $> 10\%$  ID and usually much  $> 10\%$  [Duncan et al., 1997]. The reason for reduced renal retention of 99mTc-BBN-122 is not known, however, this result demonstrates a substantial improvement over existing radiometallated peptides.

Biodistribution studies also demonstrated another important in vivo property of 99mTc-BBN-122 in that it is efficiently cleared from organs and tissues that do not express GRP receptors (or those that do not have their GRP-receptors accessible to circulating

blood). The biodistribution studies in mice demonstrated specific uptake of <sup>99m</sup>Tc-BBN-122 in the pancreas while other non-excretory organs or tissues (i.e., heart, brain, lung, muscle, spleen) exhibited little or no uptake or retention. <sup>99m</sup>Tc-BBN-122 is removed from the blood stream by both the liver and kidneys with a large fraction of the <sup>99m</sup>Tc removed by these routes being excreted into the intestines and the bladder, respectively. It is important to note that the % ID/gm in the pancreas of <sup>99m</sup>Tc-BBN-122 is 12.63%/gm at 1 hour and drops to only 5.05% at the 4 hour PI (Table C). Thus, the ratios of % ID/gm of <sup>99m</sup>Tc-BBN-122 in the pancreas relative to muscle and blood were 92.2 and 14.78 at 4 hour PI, respectively. These data demonstrated selective in vivo targeting of this <sup>99m</sup>Tc-labeled BBN analogue to cells expressing GRP receptors [Zhu et al., 1991; Qin et al., 1994] and efficient clearance from non-target tissues. If cancer cells that express GRP receptors are present in the body, these results indicate <sup>99m</sup>Tc-BBN analogues will be able to target them with a selectivity similar to the pancreatic cells.

#### EXAMPLE 9: Materials and Methods For Examples 9 and 10

The following abbreviations are used in the examples and derived from the following amino acids:

ava = 5-amino valeric acid

aoc = 8-amino octanoic acid

aun = 11-amino undecanoic acid

Reagents and Apparatus. All chemicals were obtained from either Aldrich Chemicals (St. Louis, MO) or Fisher Scientific (Pittsburgh, PA). All chemicals and solvents used in these studies were reagent grade and used without further purification. The Resin and fmoc-protected amino acids were purchased from Calbiochem-Novabiochem Corp (San Diego, CA) and the other peptide reagents from Applied Biosystems, Inc (Foster City, CA). The DOTA-tris(t-butyl ester) was purchased from Macrocyclics (Dallas, TX) and the fmoc-protected w-amino alkyl carboxylic acids from Advanced ChemTech (Louisville, KY). 1251-Tyr4-Bombesin (1251-Tyr4-BBN) was obtained from NEN Life Sciences Products, Inc (Boston, MA). <sup>111</sup>InC13 was obtained from Mallinckrodt Medical, Inc (St. Louis, MO) as a 0.05N HCl solution. <sup>90</sup>Y was obtained from Perkin-Elmer (Biclerica, MA) as an HCl solution. Electrospray mass spectral analyses were performed by Synpep Corporation and T47D (Dublin, CA). Human prostate cancer PC-3 cells and MDA-MB-231 breast cancer cells were obtained from American Tissue Culture Collection (ATCC) and maintained and grown in the University of Missouri Cell and Immunology Core facilities. CF-1 mice were purchased from Charles River Laboratories (Wilmington, MA) and maintained in an in house animal facility.

Solid Phase Peptide Synthesis (SPPS). Peptide synthesis was carried out on a Perkin Elmer - Applied Biosystems Model 432 automated peptide synthesizer employing

traditional fmoc chemistry with HBTU activation of carboxyl groups on the reactant with the N-terminal amino group on the growing peptide anchored via the C-terminus to the resin. Rink Amide MBHA resin (25  $\mu$ mol), fmoc-protected amino acids with appropriate side-chain protections (7  $\mu$ mol), fmoc-protected amino alkyl carboxylic acids (75  $\mu$ mol) and DOTA-tris(t-butyl ester) (75  $\mu$ mol) were used for the synthesis. The final products were cleaved by a standard procedure using a cocktail containing thioanisole, water, ethanedithiol and trifluoroacetic acid in a ratio of 2:1:1:36 and precipitated into methyl-t-butyl ether. Typical yields of the crude peptides were 80-85%. Crude peptides were purified by HPLC and the solvents were removed on a SpeedVac concentrator. The purified peptides were characterized by electrospray mass spectrometry. The mass spectral analysis results are shown in Table 4.

High performance liquid chromatography (HPLC). High performance liquid chromatography (HPLC) analyses for DOTA conjugates were performed on a Waters 600E system equipped with Varian 2550 variable absorption detector, Packard Radiometric 150TR flow scintillation analyzer, sodium iodide crystal radiometric detector, Eppendorf TC-50 column temperature controller and Hewlett Packard HP3395 integrators. A Phenomenex Jupiter C-18 (5 $\mu$ m, 300 Å, 4.6 X 250 mm) column was used with a flow rate of 1.5 ml/minute. HPLC solvents consisted of H<sub>2</sub>O containing 0.1 % trifluoroacetic acid (Solvent A) and acetonitrile containing 0.1% trifluoroacetic acid (Solvent B). HPLC gradient conditions for 0 spacer to 8 carbon spacer analogs begin with a solvent composition of 80% A and 20% B followed by a linear gradient to 70% A:30% B over 30 minutes. HPLC gradient conditions for the 11 carbon spacer analysis are solvent composition of 75% A and 25% B followed by a linear gradient to 50% A:50% B over 30 minutes.

*Indium metallation.* A solution of the unmetallated DOTA-BBN conjugates as shown in table 4 (5.0 mg) in 0.2M tetramethylammonium acetate (0.5 ml) was added to indium trichloride (InCl<sub>3</sub>) (10.0 mg). The pH of the reaction mixture was adjusted to 5.5 (Scheme 1). The reaction mixture was incubated for 1 hour at 80 °C. The resultant In-DOTA-BBN conjugate (Scheme 1) was purified by reversed-phase HPLC and analyzed by electrospray mass spectrometry. The mass spectral analysis results are shown in Table 4. The pure product was obtained as a white powder with a typical yield of 50-60%.

*<sup>111</sup>Indium/<sup>90</sup>Yttrium labeling.* An aliquot of <sup>111</sup>InCl<sub>3</sub> (1.0 mCi, 50  $\mu$ l) was added to a solution of the unmetallated DOTA-BBN (100  $\mu$ g) conjugates shown in Table 4 in 0.2M tetramethylammonium acetate (500  $\mu$ l). The pH of the reaction mixture was adjusted to 5.6. The reaction mixture was incubated for 1 hour at 80 °C. An aliquot of 0.002M EDTA (50  $\mu$ l) was added to the reaction mixture to complex the unreacted <sup>111</sup>In<sup>3+</sup>. The resultant <sup>111</sup>In-DOTA-BBN conjugate was obtained as a single product and purified by reversed-phase

HPLC. The purified <sup>111</sup>In-DOTA-BBN conjugate was then concentrated by passing through a 3M Empore C-18 HD high performance extraction disk (7mm/3ml) cartridge and eluting with 33% ethanol in 0.1M NaH<sub>2</sub>PO<sub>4</sub> buffer (400 µl). The concentrated fraction was then diluted with 0.1M NaH<sub>2</sub>PO<sub>4</sub> buffer (2.3 ml, pH-7) to make the final concentration of ethanol in the solution <5%. The 90Y DOTA-BBN complex was similarly prepared.

*In Vitro Cell Binding Studies.* The IC<sub>50</sub> of the various In-DOTA-BBN conjugates was determined by a competitive displacement cell binding assay using 125I-Tyr4-BBN. Briefly 3 X 10<sup>4</sup> cells suspended in RPMI medium 1640 at pH-7.4 containing 4.8 mg/ml HEPES, 0.1 µg/ml Bacitracin and 2 mg/ml BSA, were incubated at 37 °C and a 5% CO<sub>2</sub> atmosphere for 40 minutes in the presence of 20,000 cpm 125I-Tyr4-BBN and increasing concentration of the In-DOTA-BBN conjugates. After the incubation, the reaction medium was aspirated and cells were washed four times with media. The radioactivity bound to the cells was counted in a Packard Riastar gamma counting system. The % 125I-Tyr4-BBN bound to cells was plotted vs. increasing concentrations of In-DOTA-BBN conjugates to determine the respective IC<sub>50</sub> values.

*Internalization and efflux studies.* In vitro studies to determine the degree of internalization of the <sup>111</sup>In-DOTA-8-Aoc-BBN[7-14]NH<sub>2</sub> conjugate were carried out by a method similar to that of described by Rogers, et al. These studies were performed by incubating 3 X 10<sup>4</sup> cells suspended in RPMI medium 1640 at pH-7.4 containing 4.8 mg/ml HEPES, 0.1 µg/ml Bacitracin and 2 mg/ml BSA, at 37 °C and a 5% CO<sub>2</sub> atmosphere for 40 minutes in presence of 20,000 cpm <sup>111</sup>In-DOTA-8-Aoc-BBN[7-14]NH<sub>2</sub> conjugate. After the incubation, the reaction medium was aspirated and cells were washed with media. The percent of cell-associated activity as a function of time (in the incubating medium at 37 °C) was determined. The percentage radioactivity trapped in the cells was determined after removing activity bound to the surface of the cells by washing with a pH-2.5 (0.2M acetic acid and 0.5M NaCl) buffer 1, 2, 3 and 4 hours afterwards.

*In vivo pharmacokinetic studies in CF-1 mice.* The biodistribution and uptake of <sup>111</sup>In-DOTA-BBN conjugates in CF-1 mice was studied. The mice (average weight, 25 g) were injected with aliquots (50-100 µl) of the labeled peptide solution (55-75 kBq) in each animal via the tail vein. Tissues and organs were excised from the animals sacrificed at 1 hour post-injection. The activity counted in a NaI counter and the percent injected dose per organ and the percent injected dose per gram were calculated. The percent injected dose (% ID) in the blood was estimated assuming a blood volume equal to 6.5% of the total body weight. Receptor blocking studies were also carried out where excess (100 µg) BBN was administered to animals along with the <sup>111</sup>In-DOTA-8-Aoc-BBN[7-14]NH<sub>2</sub>.



*In vivo pharmacokinetic studies in human tumor bearing SCID mice.* The

biodistribution studies of the  $^{111}\text{In}$  and  $^{90}\text{Y}$  conjugates were determined in SCID mice bearing human tumor xenografts of either PC-3 (human androgen independent prostate cancer cell origin) or MDA-MB-231 (human breast cancer cell origin) cell lines. The xenograft models were produced by bilateral flank inoculation of  $5 \times 10^6$  cells (PC-3 or MDA-MB-231 cells) per site. Four to six weeks post inoculation, palpable tumors were observed. At this point, the mice were injected with  $4\mu\text{Ci}$  of the complex in  $100\mu\text{L}$  of isotonic saline via the tail vein. The mice were euthanized and tissues and organs were excised from the animals at selected times post-injection (p.i.), including 15 minutes, 30 minutes, 1 hour, 4 hours, 24 hours, 48 hours, and 72 hours p.i. Subsequently, the tissues and organs were weighed and counted in a NaI well counter and the percent injected dose (%ID) and %ID/g of each organ or tissue calculated. The %ID in whole blood was estimated assuming a whole-blood volume of 6.5% the total body weight.

*In vivo pre-clinical evaluation of single dose radiotherapy in human tumor*

bearing SCID mice. Preclinical therapeutic evaluation of the  $^{90}\text{Y}$ -DOTA-8-Aoc-BBN[7-14]NH<sub>2</sub> conjugate was performed in SCID mice bearing PC-3 human androgen independent prostate cancer cell human tumor xenografts. The xenograft model was produced by bilateral flank inoculation of  $5 \times 10^6$  PC-3 cells per site. Twenty one days post inoculation when palpable tumors appeared, single dose administration of  $^{90}\text{Y}$ -DOTA-8-Aoc-BBN[7-14]NH<sub>2</sub> was initiated. Baseline weights, hematology profiles, and tumor measurements were obtained immediately prior to therapy administration. Four groups of animals were utilized; a saline placebo, a 5 mCi/kg single dose, a 10 mCi/kg single dose, and a 20 mCi/kg single dose. Tumor measurements and weights were obtained twice weekly throughout the 14 weeks post injection.

Discussion

A series of BBN-agonists containing the DOTA chelation system separated by spacers have been synthesized and characterized. [Figures 27 and 28; Tables 4 and 20]

The in vitro binding affinity of the Indium-BBN analogs was measured in two cell lines, the human prostate cancer cell line, PC-3, and the human breast cancer cell line, T47D. Of the compounds tested, optimum binding of the  $^{111}\text{In}$ -DOTA-8-Aoc-BBN[7-14]NH<sub>2</sub> analog was demonstrated in both cell lines examined. [Figure 29 & Table 5]

The  $^{111}\text{In}$ -DOTA-8-Aoc-BBN[7-14]NH<sub>2</sub> analog underwent rapid receptor mediated endocytosis using an in vitro PC-3 cell assay system. Once internalized within PC-3 cells, the  $^{111}\text{In}$ -DOTA-8-Aoc-BBN[7-14]NH<sub>2</sub> analog remained retained within the cells for a prolonged time period. [Figures 30 and 31]

In vivo analysis of the DOTA-BBN analogs in CF1 mice demonstrates that <sup>111</sup>In-DOTA-5-Ava-BBN[7-14]NH<sub>2</sub>, <sup>111</sup>In-DOTA-8-Aoc-BBN[7-14]NH<sub>2</sub>, <sup>111</sup>In-DOTA-I 1-Aun-BBN[7-14]NH<sub>2</sub> all target GRP receptor expression in vivo based on high uptake and accumulation of these compounds in the normal pancreas. Increasing hydrocarbon spacer length linking the DOTA metal chelation moiety to the GRP receptor binding moiety (BBN[7-14]NH<sub>2</sub>) results in compounds with increased hydrophobicity which subsequently shifts the clearance of these agents from the renal system (hydrophilic agents) to the hepatobiliary system (hydrophobic agents). [Tables 6 and 7]

Specific in vivo GRP receptor binding was demonstrated by performing competitive blocking assays in CF1 normal mice, where >98% of the normal receptor mediated uptake of <sup>111</sup>In-DOTA-8-Aoc-BBN[7-14]NH<sub>2</sub> in normal pancreatic tissue was blocked by co-administration of an excess of bombesin. [Tables 8 and 9]

Prolonged PC-3 human prostate tumor uptake was demonstrated for <sup>111</sup>In-DOTA-8-Aoc-BBN[7-14]NH<sub>2</sub> and <sup>90</sup>Y-DOTA-8-Aoc-BBN[7-14]NH<sub>2</sub> using a xenograft mouse model. [Tables 10-13]

Prolonged MDA-MB-231 human breast tumor uptake was demonstrated for <sup>111</sup>In-DOTA-8-Aoc-BBN[7-14]NH<sub>2</sub> using a xenograft mouse model. [Table 14]

These in vivo pharmacokinetic studies in CF1 mice have demonstrated that the radiometallated bombesin analogues (<sup>111</sup>In and <sup>90</sup>Y) clear from the blood pool, into the renal-urinary excretion pathway.

#### Competitive Binding Assay Results

The <sup>111</sup>In and <sup>90</sup>Y complexes of one lead candidate, DOTA-8-Aoc-BBN[7-14]NH<sub>2</sub>, have been synthesized and evaluated in vitro and in vivo. In vitro competitive binding assays, employing PC-3 human prostate tumor cells, demonstrated an average IC<sub>50</sub> value of 1.69 nM for the In-DOTA-8-Aoc-BBN[7-14]NH<sub>2</sub> complex.

#### In Vivo Pharmacokinetic Results in PC-3 Tumor Bearing Mice

In vivo pharmacokinetic studies of <sup>111</sup>In-DOTA-8-Aoc-BBN[7-14]NH<sub>2</sub> in PC-3 prostate tumor bearing mice conducted at 1,4,24,48, and 72 hours p.i. revealed efficient clearance from the blood pool ( $0.92 \pm 0.58$  % ID, 1 hour p.i.) with excretion through the renal and hepatobiliary pathways (87% ID and 8.5% ID, at 24 hours p.i., respectively). Similar pharmacokinetic properties were observed with <sup>90</sup>Y-DOTA-8-Aoc-BBN[7-14]NH<sub>2</sub>. Tumor targeting of PC-3 xenografted SCID mice resulted in tumor uptake and retention values of  $3.63 \pm 1.11$ %ID/g,  $1.78 \pm 1.09$ %ID/g, and  $1.56 \pm 0.45$ %ID/g obtained at 1,4, and 24 hours p.i. respectively, for the <sup>111</sup>In-DOTA-8-Aoc-BBN-[7-14]NH<sub>2</sub> complex. <sup>90</sup>Y-DOTA-8-Aoc-BBN[7-14]NH<sub>2</sub> exhibited nearly identical PC-3 tumor uptake and retention values of  $2.95 \pm 0.99$ %ID/g,  $1.98 \pm 0.66$ %ID/g, and  $1.08 \pm 0.37$ %ID/g at 1, 4, and 24 hr p.i., respectively. Initial

therapeutic assessment of the 90Y complex in PC-3 xenografted mice demonstrated that radiation doses of up to 20mCi/kg were well tolerated with overall survival exhibiting a dose dependent response.

5. These pre-clinical observations show that peptide conjugates of this type exhibit properties suitable as clinical therapeutic/diagnostic pharmaceuticals.

#### EXAMPLE 10 Binding of DOTA-BBN Conjugates in Human Breast Cancer Cell Lines

- Expression of Gastrin Releasing Peptide receptors (GRP-Rs) in a variety of cancers including breast, prostate, small cell lung, and pancreatic is well known. Recently, the first positive clinical images of GRP-R expression in human metastatic breast cancer patients were obtained [C. Van de Wiele et al., Eur. J. Nucl. Med. (2000) 27:1694-1699] with the compound, 99mTc-N3S-5-Ava-BBN(7-14)NH<sub>2</sub>, initially developed in our laboratory. The continued efforts in the development of GRP targeted radiopharmaceuticals has led to the synthesis of a series of DOTA incorporated peptides for the complexation of 111In/90Y.

- Methods: Six synthetic peptides were constructed in an X-Y-Z fashion where X = the DOTA chelation system, Y = the linking arm, and Z = the BBN(7-14)NH<sub>2</sub> sequence. The six peptides differed in the selection of linking arms, comprising either amino acid tethers; -G-G-G-, -G-S-G-, or S-G-S-, or alkyl carbon chain tethers; 5-Ava, 8-Aoc, or 11-Aun. The In complexes of all peptides were prepared, purified by RPHPLC, and characterized by ES-MS as described in example 9.

- Results: Pharmacokinetic studies conducted in CF1 mice revealed that 111In-DOTA-8-Aoc-BBN(7-14)NH<sub>2</sub> exhibited optimum clearance kinetics while maintaining selective and high in vivo GRP receptor targeting. 111In-DOTA-8-Aoc-BBN(7-14)NH<sub>2</sub> exhibited an IC<sub>50</sub> value of 1.23 ± 0.25nM for the GRP receptor expressed by the T47D human breast cancer cell line. Pharmacokinetic studies of 111In-DOTA-8-Aoc-BBN(7-14)NH<sub>2</sub> conducted in MDA-MB-231 human breast cancer cell line xenografted SCID mice demonstrated specific tumor targeting with 0.83 ± 0.23% ID/g obtained at 1 hour post injection. Residualization of the radiolabel within the tumor was observed with 46%, and 28%, of the initial uptake retained at 4, and 24 hours, respectively.

- Conclusion: These results show that GRP-R specific radiopharmaceuticals incorporating the DOTA chelation system are beneficial for the development of diagnostic/therapeutic matched pair agents to target breast cancer.

#### EXAMPLE 11 Lutetium DOTA-BBN Compounds

- A conjugate, 177Lu-DOTA-8-Aoc-BBN[7-14]NH<sub>2</sub>, was routinely prepared in high yield (≥95%) by addition of 177LuCl<sub>3</sub> to an aqueous solution (Ammonium Acetate) of DOTA-8-Aoc-BBN[7-14]NH<sub>2</sub> (3.4x10<sup>-8</sup> mols) [pH = 5.5, Temp. = 80°C, RT = 1 hour]. RCP determination demonstrated the stability of the conjugate over a wide range of pH values over

09847134 "073001  
1.00E+00" 4ET 24860

a time course of 24 hours. The HPLC chromatogram of  $^{177}\text{Lu}$ -DOTA-8-Aoc-BBN[7-14]NH<sub>2</sub> showed a retention time of 19.0 minutes. Under identical chromatographic conditions, DOTA-8-Aoc-BBN[7-14]NH<sub>2</sub> has a retention time of 20.5 minutes, allowing for peak purification of the radiolabeled conjugate. Collection of and counting of the  $^{177}\text{Lu}$ -DOTA-8-Aoc-BBN[7-14]NH<sub>2</sub> eluant peak in a NaI well counter further demonstrated the stability of the new complex as  $\geq 95\%$  of the activity loaded onto the column was recovered as a singular species.

The biodistribution studies of  $^{177}\text{Lu}$ -DOTA-8-Aoc-BBN[7-14]NH<sub>2</sub> were determined in tumor bearing (PC-3), SCID mice (TABLE 19). This  $^{177}\text{Lu}$ -conjugate cleared efficiently from the bloodstream within 1 hour post-injection. For example,  $0.62 \pm 0.44\%$  ID remained in whole blood at 1 hour p.i. The majority of the activity was excreted via the renal-urinary excretion pathway (i.e.,  $67.41 \pm 2.45\%$  at 1 hour p.i. and  $85.9 \pm 1.4\%$  at 24 hour p.i.), with the remainder of the radioactivity being excreted through the hepatobiliary pathway. Receptor-mediated, tumor targeting of the PC-3 xenografted SCID mice resulted in tumor uptake and retention values of  $4.22 \pm 1.09\%$  ID/g,  $3.03 \pm 0.91\%$  ID/g, and  $1.54 \pm 1.14\%$  ID/g at 1, 4, and 24 hours, respectively.

EXPERIMENTAL: To  $50\mu\text{g}$  ( $3.4 \times 10^{-8}$  mols) of DOTA-8-Aoc-BBN[7-14]NH<sub>2</sub> in  $50\mu\text{L}$  of 0.2M Ammonium Acetate was added  $150\mu\text{L}$  of 0.4M Ammonium Acetate. To this solution was added  $50\mu\text{L}$  of  $^{177}\text{LuCl}_3$  (2mCi in 0.05N HCl, Missouri University Research Reactor). The solution was allowed to incubate at  $80^\circ\text{C}$  for 1 hour, after which  $50\mu\text{g}$  of 0.002M EDTA was added in order to scavenge uncomplexed Lutetium. Quality control of the final product was determined by reversed-phase HPLC. Peak purification of the labeled species was performed by collecting the sample from the HPLC eluant, into a solution of 1mg/mL bovine serum albumin/0.1M Na<sub>2</sub>HPO<sub>4</sub>. All further analyses were carried out using the HPLC-purified products.

HPLC analysis of each of the new compounds was performed using an analytical C-18 reversed phase column (Phenomenex, 250x4.6mm,  $5\mu\text{m}$ ). The mobile phase consisted of a linear gradient system, with solvent A corresponding to 100% water with 0.1% trifluoroacetic acid and solvent B corresponding to 100% acetonitrile with 0.1% trifluoroacetic acid. The mobile phase started with solvent compositions of 80%A:20%B. At time = 30 minutes, the solvent compositions were 70%A:30%B. Solvent compositions of the mobile phase remained as such (70%A:30%B) for a period of two minutes before being changed to 100%B. At time = 34 minutes, the solvent composition was again changed to 80%A:20%B for column re-equilibration. The flow rate of the mobile phase was 1.5mL/min. The chart speed of the integrator was 0.5cm/min. The results of these analyses are shown in Table 20.



In vivo analysis of the DOTA-BBN analogs in CF1 mice demonstrates that 149Pm-DOTA-5-Ava-BBN[7- 14]NH<sub>2</sub> and 149Pm-DOTA-8-Aoc-BBN[7- 14]NH<sub>2</sub> target GRP receptor expression in vivo based on high uptake and accumulation of these compounds in the normal pancreas, which contain high levels of the GRP receptor [Tables 15 and 16]

In vivo analysis of the DOTA-BBN analogs in CF1 mice demonstrates that 177Lu-DOTA-5-Ava-BBN[7- 14]NH<sub>2</sub>, 177Lu-DOTA-8-Aoc-BBN[7- 14]NH<sub>2</sub>, and 177Lu - DOTA-11-Aun-BBN[7-14]NH<sub>2</sub> all target GRP receptor expression in vivo based on high uptake and accumulation of these compounds in the normal pancreas. [Tables 17 and 18]

The biodistribution studies of 177Lu-DOTA-8-Aoc-BBN[7-14]NH<sub>2</sub> were determined in SCID mice bearing human prostate cancer, PC-3 tumors. The mice were injected with 4μCi of the complex in 100μL of isotonic saline via the tail vein. The mice were euthanized by cervical dislocation. Tissues and organs were excised from the animals following at 1 hour, 4 hour, and 24 hours post-injection (p.i.). Subsequently, the tissues and organs were weighed and counted in a NaI well counter and the percent injected dose (%ID) and %ID/g of each organ or tissue calculated. The %ID in whole blood was estimated assuming a whole-blood volume of 6.5% the total body weight.

Prolonged PC-3 human prostate tumor uptake was demonstrated for 177Lu-DOTA-8-Aoc-BBN[7-14] using a xenograft mouse model of human prostate cancer. [Table 19 and 20]

CONCLUSION: This pre-clinical evaluation of 177Lu-DOTA-8-Aoc-BBN[7-14]NH<sub>2</sub> and 149Pm-DOTA-8-Aoc-BBN[7-14]NH<sub>2</sub> suggests the potential for peptide conjugates of this type to be used as site-directed, therapeutic radiopharmaceuticals.

Table B. Biodistribution of 99mTc-BBN-122 in normal CF-1 mice at 0.5, 1, 4 and 24 hr post-IV injection. Results expressed as % ID/organ

Organ <sup>c</sup>	%Injected Dose/Organ <sup>a</sup>			
	30 min	1 hr	4 hr	24 hr
Blood <sup>d</sup>	3.52 ± 2.16	1.08 ± 0.34	0.59 ± 0.24	0.12 ± 0.01
Liver	4.53 ± 0.93	4.77 ± 1.40	1.49 ± 0.32	0.32 ± 0.06
Stomach	2.31 ± 0.45	1.61 ± 0.81	1.75 ± 0.20	0.30 ± 0.06
Lg. Intestine <sup>b</sup>	2.84 ± 0.32	24.17 ± 7.91	23.85 ± 7.02	0.61 ± 0.14

Sm. Intestine <sup>b</sup>	43.87 ± 1.51	23.91 ± 9.08	5.87 ± 7.09	0.42 ± 0.06
Kidneys <sup>b</sup>	1.49 ± 0.19	1.15 ± 0.10	0.55 ± 0.06	0.20 ± 0.01
Urine <sup>b</sup>	26.78 ± 1.05	33.79 ± 1.76	~35	~35
Muscle	0.02 ± 0.01	0.01 ± 0.00	0.01 ± 0.01	0.01 ± 0.01
Pancreas	5.30 ± 0.63	3.20 ± 0.83	1.21 ± 0.13	0.42 ± 0.17

- Each value in the table represents the mean and SD from 5 animals in each group
- At 4 and 24 hr, feces containing <sup>99</sup>Tc had been excreted from each animal and the % ID in the urine was estimated to be approximately 60% of the ID.
- All other organs excised (incl. Brain, heart, lung and spleen) shown < 0.10% at t ≥ 1 hr.
- % ID in the blood estimated assuming the whole blood volume is 6.5% of the body weight.

Table C. Biodistribution of <sup>99m</sup>Tc-BBN-122 in normal CF-1 mice at 0.5, 1, 4 and 24 hr post I.V. injection. Results expressed as % ID/gm.

Organ	%Injected Dose/gma			
	30 min	1 hr	4 hr	24 hr
Blood <sup>b</sup>	2.00 ± 1.28	0.63 ± 0.19	0.34 ± 0.11	0.08 ± 0.00
Liver	2.70 ± 0.41	3.14 ± 0.81	0.96 ± 0.20	0.22 ± 0.05
Kidneys	3.99 ± 0.76	3.10 ± 0.31	1.58 ± 0.15	0.64 ± 0.07
Muscle	0.23 ± 0.08	0.13 ± 0.02	0.05 ± 0.01	0.01 ± 0.01
Pancreas	16.89 ± 0.95	12.63 ± 1.87	5.05 ± 0.42	1.79 ± 0.71
P/B1 and P/M Update Ratios				
Pancreas/Blood	8.42	19.76	14.78	20.99

Pancreas/Muscle	73.16	93.42	92.25	142.76
-----------------	-------	-------	-------	--------

- Each value in the table represents the mean and SD from 5 animals in each group.
- % ID in the blood estimated assuming the whole blood volume is 6.5% of the body weight.

Table D. Biodistribution of  $^{99m}\text{Tc}$ -BBN-122 in PC-3 tumor bearing SCID mice at 1, 4 and 24 hr post-I.V. injection. Results expressed as % ID/organ.

Tumor Line: PC-3	% ID per Organ <sup>a</sup>		
Organ <sup>c</sup>	1 hr	4 hr	24 hr
Blood <sup>b</sup>	1.16 $\pm$ 0.27	0.47 $\pm$ 0.06	0.26 $\pm$ 0.05
Liver	1.74 $\pm$ 0.64	0.72 $\pm$ 0.10	0.29 $\pm$ 0.05
Stomach	0.43 $\pm$ 0.18	0.29 $\pm$ 0.22	0.08 $\pm$ 0.02
Lg. Intestine	9.18 $\pm$ 19.42	42.55 $\pm$ 8.74	0.64 $\pm$ 0.17
Sm. Intestine	46.55 $\pm$ 16.16	2.13 $\pm$ 0.76	0.31 $\pm$ 0.04
Kidneys	1.16 $\pm$ 0.20	0.60 $\pm$ 0.06	0.16 $\pm$ 0.01
Urine <sup>d</sup>	32.05 $\pm$ 12.78	~35	~35
Muscle	0.01 $\pm$ 0.00	0.00 $\pm$ 0.00	0.00 $\pm$ 0.00
Pancreas	1.69 $\pm$ 0.61	1.05 $\pm$ 0.13	0.34 $\pm$ 0.08
Tumor	1.00 $\pm$ 0.78	0.49 $\pm$ 0.08	0.49 $\pm$ 0.25

- Each value in the table represents the mean and SD from 5 animals in each group.
- At 4 and 24 hr, feces containing  $^{99m}\text{Tc}$  had been excreted from each animal and the % ID in the urine was estimated to be approximately 60% of the ID.
- All other organs excised (incl. brain, heart, lung and spleen) showed < 0.10% at  $t \geq 1$  hr.
- % ID in the blood estimated assuming the whole blood volume is 6.5% of the body weight.

Table E. Biodistribution of  $^{99m}\text{Tc}$ -EBN-122 in PC-3 tumor bearing SCID mice at 1, 4 and 24 hr post-I.V. injection. Results expressed as % ID/Gm.

Tumor Line: PC-3	% ID per gm <sup>a</sup>		
Organ	1 hr	4 hr	24 hr
Blood <sup>b</sup>	$0.97 \pm 0.26$	$0.31 \pm 0.03$	$0.18 \pm 0.04$
Liver	$2.07 \pm 0.88$	$0.64 \pm 0.05$	$0.26 \pm 0.04$
Kidneys	$4.80 \pm 1.33$	$2.23 \pm 0.35$	$0.60 \pm 0.04$
Muscle	$0.18 \pm 0.12$	$0.06 \pm 0.03$	$0.05 \pm 0.04$
Pancreas	$10.34 \pm 3.38$	$5.08 \pm 1.12$	$1.47 \pm 0.23$
Tumor	$2.07 \pm 0.50$	$1.75 \pm 0.61$	$1.28 \pm 0.22$
T/BI, T/M, P/BI and P/M Uptake Ratios			
Tumor/Blood	2.13	5.52	6.79
Tumor/Muscle	11.44	25.38	21.62
Pancreas/Blood	10.64	15.96	7.81
Pancreas/Muscle	57.14	73.40	24.87

- a. Each value in the table represents the mean and SD from 5 animals in each group.  
b. % ID in the blood estimated assuming the whole blood volume is 6.5% of the body weight.



The invention has been described in an illustrative manner, and it is to be understood that the terminology which has been used is intended to be in the nature of words of description rather than of limitation.

Obviously, many modifications and variations of the present invention are possible in light of the above teachings. It is, therefore, to be understood that within the scope of the appended claims the invention may be practiced otherwise than as specifically describe.

Throughout this application, various publications are referenced by citation and number. Full citations for the publication are listed below. the disclosure of these publications in their entireties are hereby incorporated by reference into this application in order to more fully describe the state of the art to which this invention pertains.



Table 1

Binding Affinity of Rh-BBN-37 for GRP Receptors  
Expressed on Neoplasms

Type of Cancer	Cell Line	IC <sub>50</sub> (Mean Value)
Pancreatic CA	CF PAC1	3.2 X 10 <sup>-9</sup>
Prostate CA	PC-3	7.0 X 10 <sup>-9</sup>

Table 2  
(%Dose)

Complex	105 Rh-Peptide22 30 min n=9	105 Rh-Peptide22 1 hr n=9	105 Rh-Peptide22 2 hr n=9
Organ (%Dose)			
Brain	0.08 ± 0.02	0.04 ± 0.01	0.06 ± 0.09
Blood	4.48 ± 1.24	1.86 ± 0.38	0.99 ± 0.24
Heart	0.13 ± 0.03	0.08 ± 0.03	0.04 ± 0.04
Lung	0.25 ± 0.08	0.20 ± 0.09	0.15 ± 0.09
Liver	7.97 ± 2.85	8.51 ± 2.33	8.57 ± 2.04
Spleen	0.07 ± 0.03	0.09 ± 0.08	0.05 ± 0.01
Stomach	1.11 ± 0.76	0.59 ± 0.21	0.30 ± 0.16
Large Intestine	0.73 ± 0.16	3.21 ± 3.38	8.91 ± 3.79
Small Intestine	6.29 ± 1.67	6.98 ± 1.87	3.48 ± 1.78
Kidneys	4.25 ± 1.33	3.25 ± 0.60	2.44 ± 0.64
Bladder	44.66 ± 7.29	62.88 ± 3.84	68.41 ± 6.63
Muscle	0.06 ± 0.03	0.03 ± 0.03	0.01 ± 0.01
Pancreas	0.95 ± 0.46	1.15 ± 0.49	1.01 ± 0.14
Carcass	32.90 ± 6.61	12.62 ± 4.77	6.37 ± 1.17

Table 2 (continued)  
(%Dose/Gm)

Complex	105 Rh-Peptide22 30 min n=9	105 Rh-Peptide22 1 hr n=9	105 Rh-Peptide22 2 hr n=9
Organ (%D/GM)			
Brain	0.21 ± 0.07	0.14 ± 0.08	0.16 ± 0.28
Blood	2.22 ± 0.40	1.02 ± 0.22	0.51 ± 0.11
Heart	0.92 ± 0.25	0.64 ± 0.20	0.38 ± 0.33
Lung	1.44 ± 0.33	1.24 ± 0.54	0.92 ± 0.69
Liver	4.33 ± 1.52	5.18 ± 1.52	5.17 ± 1.12
Spleen	0.86 ± 0.38	1.10 ± 0.65	0.84 ± 0.53
Stomach	2.46 ± 1.65	1.53 ± 0.74	0.71 ± 0.33
Large Intestine	0.78 ± 0.19	4.42 ± 4.62	10.10 ± 4.58
Small Intestine	4.73 ± 1.47	5.84 ± 1.81	2.86 ± 1.47
Kidneys	7.57 ± 1.49	6.70 ± 0.75	4.60 ± 0.83
Muscle	0.53 ± 0.32	0.61 ± 0.97	0.24 ± 0.24
Pancreas	3.12 ± 0.99	4.31 ± 1.98	3.88 ± 1.25

Table 3  
(%Dose)

Complex	105 Rh-Pept37 30 min n=5	105 Rh-Pept37 1 hr n=9	105 Rh-Pept37 2 hr n=7
Organ (%Dose)			
Brain	0.03 ± 0.01	0.07 ± 0.11	0.03 ± 0.03
Blood	3.09 ± 0.54	1.46 ± 0.62	0.66 ± 0.26
Heart	0.12 ± 0.03	0.05 ± 0.03	0.04 ± 0.02
Lung	0.26 ± 0.09	0.12 ± 0.07	0.08 ± 0.11
Liver	13.04 ± 1.93	13.00 ± 3.59	10.12 ± 1.86
Spleen	0.21 ± 0.13	0.16 ± 0.08	0.10 ± 0.04
Stomach	0.80 ± 0.34	0.65 ± 0.52	0.83 ± 0.96
Large Intestine	2.05 ± 0.69	2.96 ± 1.67	8.07 ± 2.25
Small Intestine	8.44 ± 1.89	11.38 ± 3.02	5.04 ± 2.27
Kidneys	7.82 ± 2.52	6.04 ± 1.68	4.57 ± 1.29
Bladder	39.65 ± 7.21	51.82 ± 7.53	62.32 ± 5.78
Muscle	0.06 ± 0.03	0.02 ± 0.01	0.02 ± 0.02
Pancreas	2.73 ± 1.14	3.63 ± 1.22	2.25 ± 1.02
Carcass	24.35 ± 7.69	9.81 ± 2.91	6.37 ± 1.73

Table 3 continued:  
(%Dose/Gm)

Complex	105 Rh-Pept37 30 min n=5	105 Rh-Pept37 1 hr n=9	105 Rh-Pept37 2 hr n=7
Organ (%D/GM)			
Brain	0.10 ± 0.05	0.26 ± 0.41	0.10 ± 0.09
Blood	1.60 ± 0.30	0.72 ± 0.31	0.34 ± 0.15
Heart	0.92 ± 0.26	0.38 ± 0.21	0.28 ± 0.17
Lung	1.52 ± 0.48	0.76 ± 0.47	0.46 ± 0.50
Liver	7.31 ± 1.15	7.65 ± 1.29	6.30 ± 1.73
Spleen	2.18 ± 1.17	1.59 ± 0.71	1.05 ± 0.44
Stomach	1.53 ± 0.67	1.63 ± 1.17	2.18 ± 2.35
Large Intestine	2.46 ± 0.70	3.80 ± 2.42	11.84 ± 4.39
Small Intestine	5.69 ± 1.26	7.85 ± 1.87	3.81 ± 2.01
Kidneys	14.28 ± 2.84	11.21 ± 3.68	8.39 ± 2.36
Muscle	0.73 ± 0.39	0.20 ± 0.14	0.39 ± 0.38
Pancreas	14.02 ± 3.23	15.54 ± 6.21	9.91 ± 5.35

Table 4

ES-MS and HPLC data of DOTA-BBN[7-14]NH<sub>2</sub> and In-DOTA-BBN[7-14]NH<sub>2</sub> analogues.

BBN Analogue	ES-MS			HPLC t <sub>r</sub> (min) <sup>a</sup>
	Mol. Formula	Calculated	Observed	
0	C <sub>59</sub> H <sub>91</sub> N <sub>17</sub> O <sub>16</sub> S	1326.5	1326.6	13.2
3	C <sub>62</sub> H <sub>96</sub> N <sub>18</sub> O <sub>17</sub> S	1397.6	1397.4	13.4
5	C <sub>64</sub> H <sub>100</sub> N <sub>18</sub> O <sub>17</sub> S	1425.7	1425.8	14.0
8	C <sub>67</sub> H <sub>106</sub> N <sub>18</sub> O <sub>17</sub> S	1467.8	1467.8	19.1
11	C <sub>70</sub> H <sub>112</sub> N <sub>18</sub> O <sub>17</sub> S	1509.8	1509.8	17.1 <sup>b</sup>
In-0	C <sub>59</sub> H <sub>88</sub> N <sub>17</sub> O <sub>16</sub> SIIn	1438.3	1438.2	12.9
In-3	C <sub>62</sub> H <sub>93</sub> N <sub>18</sub> O <sub>17</sub> SIIn	1509.4	1509.6	12.7
In-5	C <sub>64</sub> H <sub>97</sub> N <sub>18</sub> O <sub>17</sub> SIIn	1536.5	1537.7	13.6
In-8	C <sub>67</sub> H <sub>103</sub> N <sub>18</sub> O <sub>17</sub> SIIn	1579.6	1579.7	19.0
In-11	C <sub>70</sub> H <sub>109</sub> N <sub>18</sub> O <sub>17</sub> SIIn	1621.6	1621.7	16.8 <sup>b</sup>

Table 5

IC<sub>50</sub> (nM) values (n = 3 or 4 separate experiments performed in duplicate) of In-DOTA-BBN[7-14]NH<sub>2</sub> analogues vs. <sup>125</sup>I-Tyr<sup>4</sup>-BBN in human prostate PC-3 cells and human breast carcinoma T47D cells.

BBN Analogue	PC-3 IC <sub>50</sub> (nM)	T47D IC <sub>50</sub> (nM)
0	110.6 ± 32.3	322 ± 54.5
β-Ala	2.1 ± 0.3	4.7 ± 0.7
5-Ava	1.7 ± 0.4	2.3 ± 1.01
8-Aoc	0.6 ± 0.1	1.3 ± 0.21
11-Aun	64.0 ± 11.2	516 ± 32.2



Table 6

<sup>111</sup>In-DOTA-SPACER-BBN[7-14]NH<sub>2</sub> biodistribution (Avg %ID/gm, n = 5) in CF1 normal mice after 1 hour post-injection.

Spacer Tissue	0	β-Ala	5-Ava	8-Aoc	11-Aun
Blood	0.10 ± 0.03	0.11 ± 0.06	0.20 ± 0.07	0.32 ± 0.09	0.34 ± 0.08
Heart	0.05 ± 0.02	0.06 ± 0.04	0.10 ± 0.04	0.05 ± 0.02	0.13 ± 0.04
Lung	0.13 ± 0.03	0.11 ± 0.08	0.20 ± 0.06	0.31 ± 0.07	0.26 ± 0.05
Liver	0.09 ± 0.01	0.11 ± 0.02	0.16 ± 0.02	0.65 ± 0.07	1.22 ± 0.25
Spleen	0.08 ± 0.02	0.37 ± 0.06	0.87 ± 0.28	1.51 ± 0.41	1.15 ± 0.38
Stomach	0.06 ± 0.03	0.30 ± 0.07	0.71 ± 0.24	1.02 ± 0.26	1.05 ± 0.25
L. Intestine	0.09 ± 0.03	1.10 ± 0.78	3.07 ± 0.86	2.66 ± 1.07	4.34 ± 1.34
S. Intestine	0.44 ± 0.64	1.01 ± 0.37	3.49 ± 0.87	4.43 ± 0.90	11.12 ± 2.07
Kidney	1.24 ± 0.14	1.40 ± 0.27	1.84 ± 0.44	2.37 ± 0.31	2.06 ± 0.31
Muscle	0.03 ± 0.02	0.03 ± 0.02	0.05 ± 0.02	0.12 ± 0.05	0.09 ± 0.03
Pancreas	0.20 ± 0.04	4.92 ± 0.37	15.78 ± 2.54	26.97 ± 3.97	26.00 ± 3.46

Table 7

<sup>111</sup>In-DOTA-SPACER-BBN[7-14]NH<sub>2</sub> biodistribution (Avg %ID, n = 5) in CF1 normal mice after 1 hour post-injection.

Spacer Tissue	0	β-Ala	5-Ava	8-Aoc	11-Aun
Blood	0.22 ± 0.07	0.23 ± 0.10	0.45 ± 0.14	0.66 ± 0.13	0.79 ± 0.20
Heart	0.01 ± 0.00	0.01 ± 0.01	0.02 ± 0.01	0.01 ± 0.00	0.02 ± 0.01
Lung	0.03 ± 0.00	0.03 ± 0.02	0.04 ± 0.01	0.07 ± 0.02	0.08 ± 0.01
Liver	0.17 ± 0.02	0.17 ± 0.03	0.26 ± 0.03	1.02 ± 0.08	2.44 ± 0.50
Spleen	0.01 ± 0.00	0.05 ± 0.00	0.11 ± 0.04	0.17 ± 0.04	0.19 ± 0.04
Stomach	0.03 ± 0.01	0.13 ± 0.02	0.37 ± 0.16	0.50 ± 0.06	0.53 ± 0.11
L. Intestine	0.10 ± 0.02	0.90 ± 0.57	2.74 ± 0.80	3.02 ± 0.33	5.54 ± 2.42
S. Intestine	0.25 ± 0.04	1.57 ± 0.65	0.11 ± 0.04	6.58 ± 1.10	17.84 ± 1.40
Kidney	0.57 ± 0.02	0.62 ± 0.10	0.75 ± 0.14	1.04 ± 0.12	1.07 ± 0.17
Urine	96.95 ± 0.37	92.41 ± 0.90	81.29 ± 1.32	71.61 ± 1.82	53.26 ± 0.90
Muscle	0.01 ± 0.00	0.01 ± 0.01	0.01 ± 0.01	0.02 ± 0.01	0.02 ± 0.01
Pancreas	0.07 ± 0.01	1.84 ± 0.35	5.57 ± 0.99	10.81 ± 0.78	11.56 ± 1.14
Carcass	1.78 ± 0.37	2.23 ± 0.36	3.15 ± 0.70	5.01 ± 0.47	7.35 ± 1.57

Table 8

<sup>111</sup>In-DOTA-BBN[7-14]NH<sub>2</sub> analogues  
biodistribution (Avg %ID/gm, n = 5) in CF1  
normal mice after 1 hour post-injection.

Analogue Tissue	8-Aoc	8-Aoc Blocking
Blood	0.32 ± 0.09	0.49 ± 0.15
Heart	0.05 ± 0.02	0.16 ± 0.06
Lung	0.31 ± 0.07	0.74 ± 0.17
Liver	0.65 ± 0.07	0.54 ± 0.13
Spleen	1.51 ± 0.41	0.15 ± 0.16
Stomach	1.02 ± 0.26	0.32 ± 0.34
L. Intestine	2.66 ± 1.07	0.16 ± 0.06
S. Intestine	4.43 ± 0.90	0.95 ± 0.18
Kidney	2.37 ± 0.31	2.19 ± 0.47
Muscle	0.12 ± 0.05	0.11 ± 0.07
Pancreas	26.97 ± 3.97	0.43 ± 0.10

Table 9

$^{111}\text{In}$ -DOTA- $\beta\text{BN}[7-14]\text{NH}_2$  analogues  
biodistribution (Avg %ID, n = 5) in CF1  
normal mice after 1 hour post-injection.

Analogue Tissue	8-Aoc	8-Aoc Blocking
Blood	$0.66 \pm 0.13$	$0.98 \pm 0.23$
Heart	$0.01 \pm 0.00$	$0.03 \pm 0.01$
Lung	$0.07 \pm 0.02$	$0.17 \pm 0.05$
Liver	$1.02 \pm 0.08$	$0.87 \pm 0.10$
Spleen	$0.17 \pm 0.04$	$0.02 \pm 0.03$
Stomach	$0.50 \pm 0.06$	$0.16 \pm 0.12$
L. Intestine	$3.02 \pm 0.33$	$0.15 \pm 0.05$
S. Intestine	$6.58 \pm 1.10$	$1.65 \pm 0.19$
Kidney	$1.04 \pm 0.12$	$0.92 \pm 0.13$
Urine	$71.61 \pm 1.82$	$88.19 \pm 1.79$
Muscle	$0.02 \pm 0.01$	$0.02 \pm 0.01$
Pancreas	$10.81 \pm 0.78$	$0.19 \pm 0.03$
Carcass	$5.01 \pm 0.47$	$7.42 \pm 1.35$

Table 10

<sup>111</sup>In-DOTA-8-Aoc-BBN[7-14]NH<sub>2</sub> biodistribution (Avg %ID/gm, n = 5) in PC-3 tumor bearing mice.

Time Tissue	15 min	30 min	1 hr	4 hrs	24 hrs	48 hrs	72 hrs
Blood	5.585 ± 2.43	1.46 ± 0.44	0.60 ± 0.39	0.27 ± 0.02	0.10 ± 0.03	0.07 ± 0.03	0.01 ± 0.02
Heart	2.20 ± 1.05	0.62 ± 0.33	0.25 ± 0.18	0.13 ± 0.06	0.05 ± 0.09	0.05 ± 0.05	0.01 ± 0.01
Lung	3.35 ± 1.22	0.94 ± 0.28	0.50 ± 0.39	0.25 ± 0.08	0.09 ± 0.07	0.06 ± 0.02	0.02 ± 0.02
Liver	2.03 ± 0.85	0.70 ± 0.21	1.34 ± 0.25	1.44 ± 0.57	0.37 ± 0.12	0.13 ± 0.04	0.07 ± 0.02
Spleen	2.21 ± 0.80	0.83 ± 0.26	1.39 ± 1.17	1.59 ± 0.27	0.46 ± 0.20	0.22 ± 0.22	0.08 ± 0.09
Stomach	3.30 ± 1.99	1.82 ± 0.44	1.99 ± 0.24	0.96 ± 0.57	0.30 ± 0.05	0.12 ± 0.03	0.05 ± 0.02
L. Intestine	8.58 ± 3.04	4.33 ± 0.44	4.29 ± 2.55	10.27 ± 2.70	2.35 ± 0.43	0.81 ± 0.20	0.45 ± 0.04
S. Intestine	7.82 ± 2.26	5.16 ± 1.06	6.80 ± 1.81	2.24 ± 0.35	0.89 ± 0.16	0.25 ± 0.06	0.12 ± 0.02
Kidney	29.03 ± 14.40	8.70 ± 2.80	5.66 ± 1.33	3.18 ± 0.43	1.18 ± 0.14	0.48 ± 0.09	0.20 ± 0.02
Muscle	1.30 ± 0.60	0.32 ± 0.12	0.08 ± 0.07	0.04 ± 0.02	0.05 ± 0.05	0.02 ± 0.04	0.01 ± 0.02
Pancreas	54.33 ± 9.70	27.87 ± 3.44	18.80 ± 10.97	16.55 ± 4.43	6.78 ± 1.15	0.77 ± 0.44	0.23 ± 0.08
Tumor	7.59 ± 2.11	4.58 ± 0.53	3.63 ± 1.11	1.78 ± 1.09	1.56 ± 0.45	0.68 ± 0.24	0.34 ± 0.10

Table 11

<sup>111</sup>In-DOTA-8-Aoc-BBN[7-14]NH<sub>2</sub> biodistribution (Avg %ID, n = 5) in PC-3 tumor bearing mice.

Time Tissue	15 min	30 min	1 hr	4 hrs	24 hrs	48 hrs	72 hrs
Blood	7.92 ± 2.03	2.47 ± 0.74	0.92 ± 0.58	0.40 ± 0.11	0.15 ± 0.04	0.12 ± 0.05	0.02 ± 0.03
Heart	0.20 ± 0.07	0.06 ± 0.02	0.03 ± 0.02	0.01 ± 0.01	0.00 ± 0.01	0.01 ± 0.01	0.00 ± 0.00
Lung	0.62 ± 0.25	0.20 ± 0.06	0.09 ± 0.07	0.05 ± 0.02	0.02 ± 0.01	0.01 ± 0.00	0.00 ± 0.00
Liver	1.85 ± 0.41	0.85 ± 0.21	1.41 ± 0.32	1.57 ± 0.72	0.40 ± 0.17	0.15 ± 0.04	0.08 ± 0.01
Spleen	0.10 ± 0.02	0.08 ± 0.03	0.09 ± 0.07	0.10 ± 0.02	0.03 ± 0.02	0.01 ± 0.01	0.01 ± 0.01
Stomach	0.98 ± 0.18	0.65 ± 0.04	0.52 ± 0.11	0.34 ± 0.23	0.09 ± 0.02	0.06 ± 0.02	0.02 ± 0.01
L. Intestine	5.84 ± 0.90	4.53 ± 0.45	2.18 ± 0.86	6.04 ± 2.05	1.46 ± 0.42	0.73 ± 0.21	0.41 ± 0.05
S. Intestine	6.98 ± 0.35	6.24 ± 0.46	7.45 ± 1.62	2.43 ± 0.56	0.98 ± 0.26	0.32 ± 0.07	0.15 ± 0.02
Kidney	7.18 ± 3.16	2.45 ± 0.78	1.81 ± 0.37	0.97 ± 0.08	0.36 ± 0.08	0.16 ± 0.04	0.06 ± 0.01
Urine	27.91 ± 10.33	62.61 ± 5.02	68.56 ± 6.96	81.83 ± 3.82	87.15 ± 4.31	91.75 ± 4.13	92.53 ± 1.09
Muscle	0.16 ± 0.06	0.05 ± 0.02	0.01 ± 0.01	0.0 ± 0.00	0.01 ± 0.01	0.00 ± 0.00	0.00 ± 0.00
Feces	-	-	-	-	6.10 ± 2.60	5.89 ± 3.81	6.23 ± 1.00
Pancreas	10.26 ± 1.44	7.37 ± 1.20	3.49 ± 2.15	3.28 ± 0.80	1.19 ± 0.49	0.17 ± 0.09	0.06 ± 0.02
Carcass	33.06 ± 5.51	12.31 ± 3.27	13.55 ± 6.05	2.92 ± 0.64	1.69 ± 0.56	0.57 ± 0.02	0.38 ± 0.06
Tumor	1.92 ± 1.22	0.99 ± 0.62	0.36 ± 0.32	0.18 ± 0.17	0.25 ± 0.13	0.08 ± 0.05	0.03 ± 0.01

Table 12

<sup>90</sup>Y-DOTA-8-Aoc-BBN[7-14]NH<sub>2</sub> biodistribution (Avg %ID/gm) in PC-3 tumor bearing mice.

Time Tissue	1 hr (n = 9)	4 hrs (n = 9)	24 hrs (n = 6)	48 hrs (n = 6)	72 hrs (n = 6)
Blood	0.34 ± 0.12	0.05 ± 0.07	0.07 ± 0.08	0.06 ± 0.08	0.06 ± 0.09
Heart	0.10 ± 0.11	0.10 ± 0.14	0.00 ± 0.00	0.14 ± 0.19	0.36 ± 0.45
Lung	0.22 ± 0.12	0.07 ± 0.07	0.01 ± 0.02	0.03 ± 0.03	0.02 ± 0.03
Liver	0.39 ± 0.29	0.18 ± 0.12	0.08 ± 0.03	0.03 ± 0.03	0.08 ± 0.11
Spleen	1.09 ± 0.67	0.35 ± 0.42	0.11 ± 0.13	0.09 ± 0.24	0.28 ± 0.26
Stomach	1.34 ± 0.64	0.55 ± 0.16	0.09 ± 0.07	0.04 ± 0.07	0.07 ± 0.03
L. Intestine	3.35 ± 1.12	5.17 ± 1.85	1.27 ± 0.92	0.77 ± 0.15	0.47 ± 0.24
S. Intestine	3.64 ± 0.82	1.66 ± 0.91	0.35 ± 0.16	0.13 ± 0.04	0.08 ± 0.05
Kidney	3.77 ± 1.41	1.68 ± 0.76	0.51 ± 0.25	0.29 ± 0.12	0.43 ± 0.29
Muscle	0.15 ± 0.19	0.07 ± 0.13	0.02 ± 0.03	0.07 ± 0.13	0.08 ± 0.19
Pancreas	24.73 ± 4.97	14.02 ± 4.89	1.80 ± 0.57	0.59 ± 0.14	0.27 ± 0.17
Tumor	2.95 ± 0.99	1.98 ± 0.66	1.08 ± 0.37	0.58 ± 0.30	0.46 ± 0.48

Table 13

<sup>90</sup>Y-DOTA-8-Aoc-BEN[7-14]NH<sub>2</sub> biodistribution (Avg %ID) in PC-3 tumor bearing mice.

Time Tissue	1 hr (n = 9)	4 hrs (n = 9)	24 hrs (n = 6)	48 hrs (n = 6)	72 hrs (n = 6)
Blood	0.56 ± 0.20	0.09 ± 0.13	0.12 ± 0.14	0.10 ± 0.14	0.11 ± 0.15
Heart	0.01 ± 0.01	0.01 ± 0.01	0.00 ± 0.00	0.02 ± 0.02	0.04 ± 0.04
Lung	0.06 ± 0.03	0.01 ± 0.01	0.00 ± 0.00	0.01 ± 0.01	0.00 ± 0.01
Liver	0.44 ± 0.34	0.19 ± 0.13	0.10 ± 0.03	0.04 ± 0.04	0.08 ± 0.11
Spleen	0.07 ± 0.04	0.02 ± 0.03	0.01 ± 0.01	0.01 ± 0.02	0.02 ± 0.01
Stomach	0.41 ± 0.12	0.18 ± 0.06	0.04 ± 0.04	0.01 ± 0.02	0.04 ± 0.02
L. Intestine	2.44 ± 0.66	3.33 ± 0.71	1.11 ± 0.75	0.47 ± 0.12	0.35 ± 0.20
S. Intestine	4.65 ± 0.98	2.06 ± 1.27	0.51 ± 0.20	0.16 ± 0.06	0.11 ± 0.07
Kidney	1.22 ± 0.46	0.54 ± 0.25	0.17 ± 0.09	0.10 ± 0.04	0.13 ± 0.07
Urine	57.73 ± 14.52	67.02 ± 16.74	67.62 ± 17.26	76.74 ± 21.06	82.97 ± 25.39
Muscle	0.02 ± 0.02	0.01 ± 0.01	0.00 ± 0.01	0.01 ± 0.02	0.01 ± 0.02
Feces	-	-	10.71 ± 8.29	6.78 ± 3.88	13.89 ± 4.48
Pancreas	5.70 ± 1.60	3.42 ± 0.82	0.44 ± 0.08	0.15 ± 0.04	0.08 ± 0.05
Carcass	0.62 ± 0.44	0.14 ± 0.11	0.04 ± 0.04	0.11 ± 0.17	0.10 ± 0.11
Tumor	0.40 ± 0.22	0.34 ± 0.22	0.16 ± 0.09	0.11 ± 0.07	0.06 ± 0.06



Table 14

In Vivo Biodistribution Analyses (%ID/g (SD), n=5) of $^{111}\text{In}$ -DOTA-8-Aoc-BBN[7-14] $\text{NH}_2$ in Tumor-Bearing Mice Models (MDA-MB-231).			
Tissue/Organ	1 hour	4 hours	24 hours
Blood	$0.35 \pm 0.08$	$0.08 \pm 0.10$	$0.02 \pm 0.03$
Heart	$0.15 \pm 0.11$	$0.03 \pm 0.05$	$0.08 \pm 0.06$
Lung	$0.31 \pm 0.09$	$0.06 \pm 0.06$	$0.05 \pm 0.05$
Liver	$0.31 \pm 0.04$	$0.15 \pm 0.09$	$0.07 \pm 0.02$
Spleen	$0.57 \pm 0.10$	$0.48 \pm 0.25$	$0.21 \pm 0.07$
Stomach	$1.49 \pm 0.68$	$0.27 \pm 0.08$	$0.33 \pm 0.10$
L. Intestine	$5.14 \pm 0.42$	$5.58 \pm 1.26$	$2.76 \pm 0.49$
S. Intestine	$5.15 \pm 0.19$	$1.52 \pm 0.19$	$0.90 \pm 0.14$
Kidney	$3.29 \pm 0.56$	$1.76 \pm 0.15$	$0.98 \pm 0.28$
Pancreas	$23.4 \pm 4.99$	$17.9 \pm 5.00$	$5.06 \pm 0.77$
Muscle	$0.08 \pm 0.05$	$0.06 \pm 0.13$	$0.03 \pm 0.05$
Tumor 1	$0.91 \pm 0.16$	$0.36 \pm 0.13$	$0.22 \pm 0.07$
Tumor 2	$0.74 \pm 0.27$	$0.40 \pm 0.23$	$0.24 \pm 0.15$
Urine (%ID)	$72.1 \pm 3.55$	$84.3 \pm 2.09$	$83.8 \pm 1.41$

Table 15

<sup>149</sup>Pm-DOTA-SPACER-BBN[7-14]NH<sub>2</sub> biodistribution (Avg %ID/gm, n = 5) in CF1 normal mice after 1 hour post-injection.

Spacer Tissue	0	β-Ala	5-Ava	8-Aoc
Blood	0.00 ± 0.00	0.21 ± 0.22	0.27 ± 0.06	0.12 ± 0.13
Heart	0.00 ± 0.00	0.17 ± 0.24	0.42 ± 0.59	0.03 ± 0.06
Lung	0.00 ± 0.00	0.34 ± 0.30	0.78 ± 1.08	0.09 ± 0.14
Liver	0.12 ± 0.10	0.15 ± 0.05	0.23 ± 0.13	0.19 ± 0.12
Spleen	0.00 ± 0.00	0.16 ± 0.31	2.37 ± 1.36	1.61 ± 0.36
Stomach	0.04 ± 0.08	0.19 ± 0.11	1.90 ± 1.60	1.16 ± 0.59
L. Intestine	0.01 ± 0.03	0.42 ± 0.08	3.53 ± 1.10	4.14 ± 2.14
S. Intestine	0.27 ± 0.17	0.63 ± 0.20	5.15 ± 1.20	12.56 ± 16.70
Kidney	1.04 ± 0.90	2.05 ± 1.63	2.81 ± 0.66	3.74 ± 1.02
Muscle	0.00 ± 0.00	0.04 ± 0.10	0.24 ± 0.25	0.09 ± 0.21
Pancreas	0.00 ± 0.00	2.40 ± 1.33	22.1 ± 5.40	28.29 ± 13.26

Table 16

$^{149}\text{Pm}$ -DOTA-SPACER-BBN[7-14] $\text{NH}_2$  biodistribution (A g %ID, n = 5) in CF1 normal mice after 1 hour post-injection.

Spacer Tissue	0	$\beta$ -Ala	5-Ava	8-Aoc
Blood	$0.00 \pm 0.00$	$0.30 \pm 0.32$	$0.47 \pm 0.11$	$0.23 \pm 0.26$
Heart	$0.00 \pm 0.00$	$0.02 \pm 0.02$	$0.06 \pm 0.09$	$0.00 \pm 0.01$
Lung	$0.00 \pm 0.00$	$0.06 \pm 0.04$	$0.17 \pm 0.21$	$0.02 \pm 0.04$
Liver	$0.16 \pm 0.15$	$0.23 \pm 0.07$	$0.37 \pm 0.20$	$0.35 \pm 0.20$
Spleen	$0.00 \pm 0.00$	$0.02 \pm 0.04$	$0.27 \pm 0.13$	$0.24 \pm 0.06$
Stomach	$0.02 \pm 0.05$	$0.10 \pm 0.03$	$0.77 \pm 0.74$	$0.66 \pm 0.35$
L. Intestine	$0.01 \pm 0.02$	$0.31 \pm 0.06$	$3.18 \pm 1.18$	$4.43 \pm 2.37$
S. Intestine	$0.38 \pm 0.25$	$0.95 \pm 0.19$	$7.70 \pm 0.66$	$7.84 \pm 2.15$
Kidney	$0.34 \pm 0.28$	$0.61 \pm 0.41$	$1.11 \pm 0.29$	$1.55 \pm 0.47$
Urine	$97.10 \pm 2.91$	$95.54 \pm 1.15$	$75.82 \pm 2.02$	$67.20 \pm 5.53$
Muscle	$0.00 \pm 0.00$	$0.00 \pm 0.01$	$0.03 \pm 0.04$	$0.01 \pm 0.02$
Pancreas	$0.07 \pm 0.01$	$0.46 \pm 0.23$	$4.25 \pm 0.43$	$7.34 \pm 3.51$
Carcass	$1.98 \pm 2.27$	$1.64 \pm 0.38$	$6.16 \pm 0.75$	$10.30 \pm 1.84$

Table 17

<sup>177</sup>Lu-DOTA-SPACER-BBN[7-14]NH<sub>2</sub> biodistribution (Avg %ID/gm, n = 5) in CF1 normal mice after 1 hour post-injection.

Spacer Tissue	0	β-Ala	5-Ava	8-Aoc	11-Aun
Blood	0.58 ± 0.96	0.16 ± 0.17	0.22 ± 0.19	0.14 ± 0.10	0.78 ± 1.10
Heart	0.04 ± 0.09	0.43 ± 0.70	0.34 ± 0.35	0.19 ± 0.36	1.56 ± 2.40
Lung	0.19 ± 0.26	0.23 ± 0.33	0.47 ± 0.84	0.20 ± 0.21	0.73 ± 0.81
Liver	0.09 ± 0.06	0.15 ± 0.06	0.09 ± 0.04	0.23 ± 0.05	1.65 ± 0.29
Spleen	0.04 ± 0.09	0.31 ± 0.31	1.26 ± 0.69	1.23 ± 0.59	1.78 ± 1.87
Stomach	0.10 ± 0.21	0.34 ± 0.18	1.48 ± 2.25	1.41 ± 0.44	1.82 ± 1.12
L. Intestine	0.07 ± 0.09	0.45 ± 0.19	3.78 ± 1.23	6.17 ± 0.79	6.31 ± 0.86
S. Intestine	0.75 ± 0.60	0.49 ± 0.10	2.55 ± 1.31	6.47 ± 1.24	12.58 ± 1.73
Kidney	1.21 ± 0.31	1.88 ± 0.37	2.03 ± 1.02	4.97 ± 0.71	4.97 ± 0.61
Muscle	0.09 ± 0.15	0.94 ± 1.54	0.67 ± 0.90	0.17 ± 0.39	0.75 ± 1.12
Pancreas	0.18 ± 0.28	1.44 ± 0.26	16.41 ± 1.38	30.83 ± 1.89	35.48 ± 2.39

Table 18

<sup>177</sup>Lu-DOTA-SPACER-BBN[7-14]NH<sub>2</sub> biodistribution (Avg %ID, n = 5) in CF1 normal mice after 1 hour post-injection.

Spacer Tissue	0	β-Ala	5-Ava	8-Aoc	11-Aun
Blood	0.39 ± 0.34	0.24 ± 0.25	0.35 ± 0.31	0.20 ± 0.15	0.47 ± 0.54
Heart	0.01 ± 0.02	0.05 ± 0.08	0.04 ± 0.05	0.02 ± 0.04	0.19 ± 0.29
Lung	0.04 ± 0.06	0.04 ± 0.06	0.08 ± 0.15	0.03 ± 0.04	0.17 ± 0.22
Liver	0.19 ± 0.10	0.21 ± 0.09	0.14 ± 0.06	0.31 ± 0.05	2.26 ± 0.46
Spleen	0.01 ± 0.01	0.05 ± 0.04	0.18 ± 0.12	0.16 ± 0.05	0.24 ± 0.24
Stomach	0.05 ± 0.11	0.13 ± 0.09	0.73 ± 1.33	0.51 ± 0.15	0.64 ± 0.35
L. Intestine	0.09 ± 0.12	0.36 ± 0.17	3.52 ± 1.37	4.63 ± 0.57	5.03 ± 0.46
S. Intestine	1.27 ± 1.03	0.64 ± 0.20	3.80 ± 1.87	9.55 ± 2.37	17.10 ± 3.60
Kidney	0.58 ± 0.10	0.63 ± 0.14	0.69 ± 0.33	1.62 ± 0.14	1.76 ± 0.25
Urine	93.26 ± 3.61	94.66 ± 1.88	84.08 ± 2.13	71.16 ± 1.05	58.76 ± 3.44
Muscle	0.02 ± 0.03	0.11 ± 0.18	0.09 ± 0.12	0.02 ± 0.05	0.11 ± 0.18
Pancreas	0.06 ± 0.10	0.32 ± 0.07	3.78 ± 1.09	7.01 ± 1.42	6.89 ± 1.20
Carcass	4.34 ± 2.64	2.73 ± 1.08	2.77 ± 0.75	4.95 ± 1.41	6.69 ± 2.48

Table 19

<sup>177</sup>Lu-DOTA-8-Aoc-BBN[7-14]NH<sub>2</sub> biodistribution (Avg %ID/gm, n = 5) in PC-3 tumor bearing mice

Time Tissue	1 hr (n = 5)	4 hrs (n = 5)	24 hrs (n = 5)
Blood	0.38 ± 0.22	0.08 ± 0.07	0.01 ± 0.01
Heart	0.15 ± 0.22	0.07 ± 0.13	0.06 ± 0.09
Lung	0.18 ± 0.09	0.11 ± 0.15	0.14 ± 0.26
Liver	0.30 ± 0.05	0.13 ± 0.02	0.03 ± 0.02
Spleen	0.33 ± 0.51	0.60 ± 0.36	0.08 ± 0.10
Stomach	1.38 ± 0.52	0.34 ± 0.34	0.19 ± 0.13
L. Intestine	3.29 ± 0.61	7.29 ± 3.73	1.90 ± 0.53
S. Intestine	5.60 ± 0.46	1.93 ± 0.96	0.48 ± 0.14
Kidney	4.70 ± 0.95	2.18 ± 0.31	0.60 ± 0.20
Muscle	0.11 ± 0.13	0.15 ± 0.21	0.10 ± 0.17
Pancreas	38.53 ± 3.61	22.18 ± 4.66	4.97 ± 2.28
Tumor	4.22 ± 1.09	3.03 ± 0.91	1.54 ± 1.14

**TABLE 20.**<sup>177</sup>Lu-DOTA-8-Aoc-BBN[7-14]NH<sub>2</sub> biodistribution (Avg %ID, n = 5) in PC-3 tumor bearing mice.

Time Tissue	1 hr (n = 5)	4 hrs (n = 5)	24 hrs (n = 5)
Blood	0.62 + 0.44	0.12 + 0.11	0.01 + 0.02
Heart	0.01 + 0.02	0.01 + 0.02	0.01 + 0.01
Lung	0.04 + 0.02	0.05 + 0.09	0.03 + 0.05
Liver	0.38 + 0.09	0.15 + 0.03	0.04 + 0.03
Spleen	0.03 + 0.04	0.05 + 0.02	0.01 + 0.01
Stomach	0.61 + 0.09	0.22 + 0.06	0.09 + 0.06
L. Intestine	3.64 + 0.72	7.28 + 4.23	1.75 + 0.23
S. Intestine	8.20 + 1.72	2.51 + 0.75	0.67 + 0.12
Kidney	1.35 + 0.41	0.61 + 0.08	0.17 + 0.06
Urine	67.41 + 2.45	79.76 + 6.48	85.85 + 1.39
Muscle	0.01 + 0.02	0.02 + 0.03	0.02 + 0.03
Pancreas	9.70 + 1.12	5.23 + 1.68	1.31 + 0.45
Tumor	1.15 + 0.72	0.78 + 0.27	0.29 + 0.18
Carcass	6.18 + 1.01	2.52 + 1.18	2.08 + 3.14



#### REFERENCES CITED

- Albert et al., (1991) Labeled Polypeptide Derivatives, Int'l Patent No. WO91/01144.
- 5    Bjisterbosch, M.K., et al., (1995) Quarterly J. Nucl. Med. 39:4-19.
- Bushbaum, (1995) Pharmacokinetics of Antibodies and Their Radiolabels. In: Cancer Therapy with Radiolabeled Antibodies, (ed) D.M. Goldenberg, CRC Press, Boca Raton, Chapter 10, 115-140 FL.
- 10    Cai et al., (1992) Peptides, 13:267.
- Cai et al., (1994) Proc. Natl. Acad. Sci., 91:12664.
- 15    Coy et al., (1988) J. Biolog. Chem., 263(11), 5066.
- Cutler, C., Hu, F., Hoffman, T.J., Volkert, W.A., and Jurisson, S.S., "DOTA Bombesin Complexes with Sm-153 and NCA PM-149", The International Chemical Congress of Pacific Basin Societies, Pacificchem 2000,, Honolulu, HI, December, 2000.
- 20    Davis et al. (1992) Peptides, 13:401.
- de Jong et al., (1997) Eur. J. Nucl. Med., 24:368.
- 25    Duncan et al., (1997) Cancer Res. 57:659.
- Eckelman (1995) Eur. J. Nucl. Med., 22:249.
- Eckelman et al., (1993) The design of site-directed radiopharmaceuticals for use in drug discovery. In: Nuclear Imaging in Drug Discovery, Development and Approval (eds) H.D. Burns et al., Birkhauser Publ. Inc., Boston, MA.
- 30    Fischman et al., (1993) J. Nucl. Med., 33:2253.
- 35    Fritzberg et al., (1992) J. Nucl. Med., 33:394.
- Fritzberg et al. (1995) Radiolabeling of antibodies for targeted diagnostics. In: Targeted Delivery of Imaging Agents (ed) V.P. Torchilin, CRC Press, Boca Raton, FL, pp. 84-101.
- 40    Gali, H., Hoffman, T.J., Owen, N.K., Sieckman, G.L., and Volkert, W.A., "In Vitro and In Vivo Evaluation of <sup>111</sup>In-Labeled DOTA\_8\_Aoc\_BBN[7\_14]NH<sub>2</sub> Conjugate for Specific Targeting of Tumors Expressing Gastrin Releasing Peptide (GRP) Receptors", 47th Annual Meeting - Society of Nuclear Medicine, St. Louis, MO, J.Nucl. Med., 41(5), 119P, #471, 2000.
- 45    Gali, H., Hoffman, T.J., Sieckman, G.L., Katti, K.V., and Volkert, W.A., "Synthesis, Characterization and Labeling with <sup>99m</sup>Tc/<sup>188</sup>Re of Peptide Conjugates Containing a Dithio-Bisphosphine Chelating Agent" Bioconjugate Chemistry (Accepted), 2001.
- 50    Gali, H., Hoffman, T.J., Sieckman, G.L., Katti, K.V., and Volkert, W.A. "Synthesis, Characterization, and Labeling with <sup>99m</sup>Tc/<sup>188</sup>Re of Peptide Conjugates Containing a Dithio-bisphosphine Chelating Agent", American Chemical Society Annual Meeting, San Francisco, CA, April, 2000.



Gali, H., Smith, C.J., Hoffman, T.J., Sieckman, G.L., Hayes, D.L., Owen, N.K., and Volkert, W.A., "Influence of the Radiometal on the In Vivo Pharmacokinetic Properties of a Radiometal-labeled DOTA-Conjugated Peptide", 222nd American Chemical Society National Meeting, Chicago, IL, August, 2001 (Accepted)

5

Hermanson (1996) In: Bioconjugate Techniques, Academic Press, pp. 3-136.

Hoffken, (ed) (1994) Peptides in Oncology II, Springer-Verlag, Berlin-Heidelberg.

10 Hoffman, et al., (1997) Quarterly J. Nucl. Med. 41(2) Supp. #1, 5.

Hoffman, T.J. and Volkert, W.A. "Design of Radiolabeled Bombesin Analogs" Receptors 2000; DOE Sponsored Workshop (La Jolla, CA) April 17-18, 2000.

15 Hoffman, T.J., Gali, H., Sieckman, G.L., Forte, L.R., Chin, D.T., Owen, N.K., Wooldridge, J.E., and Volkert, W.A., "Development and Characterization of a Receptor-Avid <sup>111</sup>In-Labeled Peptide for Site-Specific Targeting of Colon Cancer", 92nd Annual Meeting of the American Association for Cancer Research, New Orleans, LA. Proceedings of the American Association for Cancer Research, Vol. 42, 139, #746, March 2001.

20

Hoffman, T.J., Li, N., Sieckman, G., and Volkert, W.A., "Uptake and Retention of a Rh-105 Labeled Bombesin Analogue in GRP Receptor Expressing Neoplasms: An In-Vitro Study", 44th Annual Meeting - Society of Nuclear Medicine, June, 1997; J.Nucl. Med., 38(5), 188P, 1997.

25

Hoffman, T.J., Li, N., Sieckman, G., Higginbotham, C.A., and Volkert, W.A., "Evaluation of Radiolabeled (<sup>111</sup>In vs. Rh-105) Bombesin Analogue Internalization in Normal and Tumor Cell Lines", 10th International Symposium on Radiopharmacology, May, 1997; Quarterly J. Nucl. Med., 41(2) Suppl#1, 5, 1997.

30

Hoffman, T.J., Li, N., Volkert, W.A., Sieckman, G., Higginbotham, C.A., and Ochrymowycz, L.A., "Synthesis and Characterization of Rh-105 Labeled Bombesin Analogues: Enhancement of GRP Receptor Binding Affinity Utilizing Aliphatic Carbon Chain Linkers", J. Label. Comp'd Radiopharm., 1997.

35

Hoffman, T.J., Li, N., Volkert, W.A., Sieckman, G., Higginbotham, C.A., and Ochrymowycz, L.A., "Synthesis and Characterization of Rh-105 Labeled Bombesin Analogues: Enhancement of GRP Receptor Binding Affinity Utilizing Aliphatic Carbon Chain Linkers", 12th International Symposium on Radiopharmaceutical Chemistry, June, 1997.

40

Hoffman, T.J., Li, N., Higginbotham, C.A., Sieckman, G., Volkert, W.A., "Specific Uptake and Retention of Rh-105 Labeled Bombesin Analogues in GRP-Receptor Expressing Cells", European Society of Nuclear Medicine, August, 1997; Eur. J. Nucl. Med., 24(8), 901, 1997.

45

Hoffman, T.J., Li, N., Sieckman, G.L., Higginbotham, C. Ochrymowycz, L.A., Volkert, W.A. "Rh-105 Bombesin Analogs: Selective In Vivo Targeting of Prostate Cancer with a Therapeutic Radionuclide", 45th Annual Meeting - Society of Nuclear Medicine, June 1998; J.Nucl. Med., 39(5), 222P, 1998.

50

Hoffman, T.J., Quinn, T.P., and Volkert, W.A., "Radiometallated Receptor-Avid Peptide Conjugates for Specific In Vivo Targeting of Cancer", Nuc. Med. & Biol. (Accepted), 2001.

Hoffman, T.J., Sieckman, G., Volkert, W.A., "Targeting Small Cell Lung Cancer Using Iodinated Peptide Analogs", J. Label. Comp'd Radiopharm., 37:321-323, 1995.

- 5 Hoffman, T.J., Sieckman, G., Volkert, W.A., "Targeting Small Cell Lung Cancer Using Iodinated Peptide Analogs", 11th International Symposium on Radiopharmaceutical Chemistry, August, 1995; J. Label. Comp'd Radiopharm., 37:321-323, 1995.

- 10 Hoffman, T.J., Sieckman, G.L., Volkert, W.A., "Iodinated Bombesin Analogs: Effect of N-Terminal Chain Iodine Attachment on BBN/GRP Receptor Binding", 43rd Annual Meeting - Society of Nuclear Medicine, June, 1996; J.Nucl. Med., 37(5), p185P, 1996.

- 15 Hoffman, T.J., Simpson, S.D., Smith, C.J., Sieckman, G.L., Higginbotham, C., Volkert, W. and Thornback, J.R. "Accumulation and Retention of 99mTc-RP527 by GRP Receptor Expressing Tumors in SCID Mice", 46th Annual Meeting - Society of Nuclear Medicine, Los Angeles, CA, J.Nucl. Med., 40(5), 104P, 1999.

- 20 Hoffman, T.J., Simpson, S.D., Smith, C.J., Sieckman, G.L., Higginbotham, C., Eshima, D., Volkert, W. and Thornback, J.R. "Accumulation and Retention of 99mTc-RP591 by GRP Receptor Expressing Tumors in SCID Mice", Congress of the European Association of Nuclear Medicine, Barcelona, Spain, Eur. J. Nucl. Med., 26(9), 1157, #PS-420, September, 1999.

- 25 Hoffman, T.J., Smith, C.J., Gali, H., Owen, N.K., Sieckman, and Volkert, W.A., "In Vitro and In Vivo Evaluation of 111In/90Y Radiolabeled Peptides for Specific Targeting of Tumors Expressing Gastrin Releasing Peptide (GRP) Receptors", 92nd Annual Meeting of the American Association for Cancer Research, New Orleans, LA. Proceedings of the American Association for Cancer Research, Vol. 42, 773, #4148, March 2001.

- 30 Hoffman, T.J., Smith, C.J., Gali, H., Owen, N.K., Sieckman, Hayes, D.L., and Volkert, W.A., "Development of a Diagnostic Radiopharmaceutical for Visualization of Primary and Metastatic Breast Cancer", 48th Annual Meeting-Society of Nuclear Medicine, Toronto, Ontario, Canada, June 2001. (Accepted)

- 35 Hoffman, T.J., Smith, C.J., Gali, H., Owen, N.K., Sieckman, Hayes, D.L., Foster, B., and Volkert, W.A., "111In/90Y Radiolabeled Peptides for Targeting Prostate Cancer; A Matched Pair Gastrin Releasing Peptide (GRP) Receptor Localizing Radiopharmaceutical", 48th Annual Meeting-Society of Nuclear Medicine, Toronto, Ontario, Canada, June 2001. (Accepted)

- 40 Hoffman, T.J., Smith, C.J., Sieckman, G.L., Owen, N.K., and Volkert, W.A., "Design, Synthesis, and Biological Evaluation of Novel Gastrin Releasing Peptide Receptor Targeting Radiopharmaceuticals" American Chemical Society Annual Meeting, August 2000, Washington, D.C.

- 45 Hoffman, T.J., Smith, C.J., Simpson, S.D., Sieckman, G.L., Higginbotham, C., Jimenez, H., Eshima, D., Thornback, J.R., and Volkert, W.A. "Targeting Gastrin Releasing Peptide Receptor (GRP-R) Expression in Prostate and Pancreatic Cancer Using Radiolabeled GRP Agonist Peptide Vectors", American Association for Cancer Research Annual Meeting, San Francisco, CA, Proceedings of the American Association for Cancer Research, Vol. 41, 529, #3374, April, 2000.
- 50

Hoffman, T.J., Smith, C.J., Simpson, S.D., Sieckman, G.L., Higginbotham, C., Jimenez, H., Eshima, D., Thornback, J.R., and Volkert, W.A., "Optimizing Pharmacokinetics of Tc-99m-

GRP Receptor Targeting Peptides Using Multi-Amino Acid Linking Groups", 47th Annual Meeting - Society of Nuclear Medicine, St. Louis, MO, J.Nucl. Med., 41(5), 228P, #1013, 2000.

5 Jensen et al., (1993) Rec. Result. Cancer Res., 129:87.

Karra, S.R., Schibli, R., Gali, H., Katti, K.V., Hoffman, T.J., Higginbotham, C., Sieckman, G., Volkert, W.A., "99mTc-Labeling and In Vivo Studies of a Bombesin Analogue with a Novel Water-soluble Dithia-Diphosphine Based Bifunctional Chelating Agent", Bioconjugate Chemistry, 10:254-260, 1999.

Katti, K.V, Gali, H., Schibli, R., Hoffman, T.J., and Volkert, W.A. "99mTc/Re Coordination Chemistry and Biomolecule Conjugation Strategy of a Novel Water Soluble Phosphine-Based Bifunctional Chelating Agent", Fifth International Symposium of Technetium in Chemistry and Nuclear Medicine, Bressanone, Italy, September, 1998.

Katti, K.V., Gali, H., Schibli, R., Hoffman, T.J., and Volkert, W.A. "99mTc/Re Coordination Chemistry and Biomolecule Conjugation Strategy of a Novel Water Soluble Phosphine-Based Bifunctional Chelating Agent", In Technetium, Rhenium and Other Metals in Chemistry and Nuclear Medicine (5), Ed. By M. Nicolini and U. Mazzi, Servizi Grafici Editoriali, Padova, pp. 93-100, 1999.

Kothari, K.K., Katti, K.V., Prabhu, K.R., Gali, H., Pillarsetty, N.K., Hoffman, T.J., Owen, N.K., and Volkert, W.A., "Development of a Diamido-Diphosphine (N2P2)-BFCA for Labeling Cancer Seeking Peptides via the 99mTc(I)(CO)3(H2O)3 Intermediate", 47th Annual Meeting - Society of Nuclear Medicine, St. Louis, MO, J.Nucl. Med., 41(5), 244P, #1079, 2000.

Krenning et al., (1994) Semin. Oncology, 5-14.

30 Leban et al. (1994) J. Med. Chem., 37:439.

Li et al., (1996a) J. Nucl. Med., 37:61P.

35 Li et al., (1996b) Radiochim Acta, 75:83.

Li, W.P., Ma, D.S., Higginbotham, C., Hoffman, T.J., Ketrin, A.R., and Jurisson, S.S., "Development of an In Vitro Model for Assessing the In Vivo Stability of Lanthanide Chelates", Nuc. Med. & Biol. 28:145-154, 2001.

40 Lister-James et al. (1997) Quart. J. Nucl. Med., 41:111.

Lowbartz et al., (1994) Semin. Oncol., 1-5.

45 Mattes, (1995) Pharmacokinetics of antibodies and their radiolabels. In: Cancer Therapy with Radiolabeled Antibodies (ed) D.M. Goldenberg, CRC Press, Boca Raton, FL

Moody et al., (1995) Life Sciences, 56(7), 521.

50 Moody et al., (1996) Peptides, 17(8), 1337.

Ning, Li, Hoffman, T.J., Sieckman, G.L., Ochrymowycz, L.A., Higginbotham, C., Struttman, M., Volkert, W.A., and Ketrin, A.R., "In-vitro and In-vivo Characterization of a Rh-105-

tetrathiamacrocyclic Conjugate of a Bombesin Analogue", 43rd Annual Meeting - Society of Nuclear Medicine, June, 1996; J. Nucl. Med., 37(5), p61P, 1996.

Parker (1990) Chem. Soc. Rev., 19:271.

5

Pollak et al., (1996) Peptide Derived Radionuclide Chelators, Int'l Patent No. WO96/03427.

Qin et al., (1994) J. Canc. Res. Clin. Oncol., 120:519.

10 Qin, Y. et al., (1994) Cancer Research 54: 1035-1041.

Reile, H. et al., (1994) Prostate 25: 29-38.

15 Schibli, R., Karra, S., Katti, K.V., Gali, H., Higginbotham, C., Sieckman, G., Hoffman, T.J., Volkert, W.A., "A Tc-99m-Dithia-Di(Bis-Hydroxy-methylene)Phosphine Conjugate of Bombesin: In Vitro and In Vivo Studies" 45th Annual Meeting - Society of Nuclear Medicine, June, 1998; J. Nucl. Med., 39(5), 225P, 1998.

20 Schibli, R., Karra, S.R., Gali, H., Katti, K.V., Higginbotham, C., Smith, C.J., Hoffman, T.J., and Volkert, W.A. "Conjugation of Small Biomolecules and Peptides with Water-Soluble Dithio-Bis-Hydroxymethylphosphine Ligands", Annual Meeting of the American Chemical Society, April, 1998.

Schubiger et al., (1996) Bioconj. Chem.

25

Seifert et al. (1998) Appl. Radiat. Isot., 49:5.

Smith et al., (1997) Nucl. Med. Biol., 24:685.

30 Smith, C.J., Hoffman, T.J., Gali, H., Hayes, D.L., Owen, N.K., Sieckman, G.L., and Volkert, W.A., "Radiochemical Investigations of <sup>177</sup>Lu-DOTA-8-Aoc-BBN(7-14)NH<sub>2</sub>: A New Gastrin Releasing Peptide Receptor (GRPr) Targeting Radiopharmaceutical", J. Labeled Compounds and Radiopharmaceuticals (Accepted), 2001

35 Smith, C.J., Hoffman, T.J., Gali, H., Hayes, D.L., Owen, N.K., Sieckman, G.L., and Volkert, W.A., "Radiochemical Investigations of <sup>177</sup>Lu-DOTA-8-Aoc-BBN(7-14)NH<sub>2</sub>: A New Gastrin Releasing Peptide Receptor (GRPr) Targeting Radiopharmaceutical", 14th International Symposium on Radiopharmaceutical Chemistry, Interlaken Switzerland, June, 2001, J. Labeled Compounds and Radiopharmaceuticals (Accepted)

40

Smythe, E. et al., (1991) Eur. J. Biochem. 202: 689-699.

Troutner (1987) Nucl. Med. Biol., 14:171.

45 Vallabhajosula et al., (1996) J. Nucl. Med., 37:1016.

Volkert, W.A., and Hoffman, T.J. "Design and Development of Receptor-avid Peptide Conjugates for In Vivo Targeting of Cancer", In Biomedical Imaging: Reporters, Dyes, and Instrumentation, Ed. by D.J. Bornhop, C.H. Contag, and E.M. Sevick\_Muraca, Proceedings of SPIE Vol. 3600, 86-98, 1999.

50

Volkert, W.A., Gali, H-P, Hoffman, T.J., Owen, N.K., Sieckman, G.L., and Smith, C.J., "<sup>111</sup>In/<sup>90</sup>Y Labeled GRP Analogs: A Structure-Activity Relationship", The International

Chemical Congress of Pacific Basin Societies, Pacificchem 2000,, Honolulu, HI, December, 2000.

- 5 Volkert, W.A., Hoffman, T.J., Li, N., Sieckman, G., Higginbotham, C., "Therapeutic Potential for Small Radiometallated Site-Specific Drugs", Radiation Research Society - Annual Meeting, May, 1997.

Wilbur (1992) Bioconj. Chem., 3:433.

- 10 Wong, E. et al., (1997) Inorg. Chem. 36: 5799-5808.

Zhu, W-Y. et al., (1991) Am. J. Physiol. 261: G57-64.